

Article

Predictive Modelling of Reference Evapotranspiration Using Machine Learning Models Coupled with Grey Wolf Optimizer

Pangam Heramb^{1,2,*}, K. V. Ramana Rao¹, A. Subeesh³ and Ankur Srivastava^{4,*}

¹ Irrigation and Drainage Engineering Division, ICAR—Central Institute of Agricultural Engineering, Bhopal 462038, India

² Outreach Program (ICAR-CIAE), ICAR—Indian Agricultural Research Institute, New Delhi 110012, India

³ Agricultural Mechanization Division, ICAR—Central Institute of Agricultural Engineering, Bhopal 462038, India

⁴ Faculty of Science, University of Technology Sydney, Sydney, NSW 2007, Australia

* Correspondence: herambpangam@gmail.com (P.H.); ankur.srivastava@uts.edu.au (A.S.)

Abstract: Mismanagement of fresh water is a primary concern that negatively impacts agricultural productivity. Judicious use of water in agriculture is possible by estimating the optimal requirement. The present practice of estimating crop water requirements is using reference evapotranspiration (ET_0) values, which is considered a standard method. Hence, predicting ET_0 is vital in allocating and managing available resources. In this study, different machine learning (ML) algorithms, namely random forests (RF), extreme gradient boosting (XGB), and light gradient boosting (LGB), were optimized using the naturally inspired grey wolf optimizer (GWO) viz. GWORF, GWOXGB, and GWOLGB. The daily meteorological data of 10 locations falling under humid and sub-humid regions of India for different cross-validation stages were employed, using eighteen input scenarios. Besides, different empirical models were also compared with the ML models. The hybrid ML models were found superior in accurately predicting at all the stations than the conventional and empirical models. The reduction in the root mean square error (RMSE) from 0.919 to 0.812 mm/day in the humid region and 1.253 mm/day to 1.154 mm/day in the sub-humid region was seen in the least accurate model using the hyperparameter tuning. The RF models have improved their accuracies substantially using the GWO optimizer than LGB and XGB models.

Keywords: evapotranspiration; grey wolf optimizer; machine learning; meta-heuristics; humid; sub-humid; random forests; boosting



Citation: Heramb, P.; Ramana Rao, K.V.; Subeesh, A.; Srivastava, A. Predictive Modelling of Reference Evapotranspiration Using Machine Learning Models Coupled with Grey Wolf Optimizer. *Water* **2023**, *15*, 856. <https://doi.org/10.3390/w15050856>

Academic Editor: Yongqiang Zhang

Received: 19 January 2023

Revised: 7 February 2023

Accepted: 20 February 2023

Published: 22 February 2023



Copyright: © 2023 by the authors. Licensee MDPI, Basel, Switzerland. This article is an open access article distributed under the terms and conditions of the Creative Commons Attribution (CC BY) license (<https://creativecommons.org/licenses/by/4.0/>).

1. Introduction

India is projected to be the World's most populous country by 2023, surpassing China, which will have to feed about 1.66 billion people by 2050 [1]. Thus, the pressure on natural resources and food systems to produce more food would become a reality. Effective planning on water resource utilization should be the objective for water resource planners. The per capita availability of water is decreasing day by day due to the increase in population. According to the Ministry of Jal Shakti, Government of India, the average annual per capita water availability was 1816 cubic meters, 1545 cubic meters, and 1487 cubic meters for 2001, 2011, and 2021, respectively. It was estimated to further deteriorate to 1367 cubic meters by 2031.

Efficient water management in agriculture is required in developing nations, which are disadvantaged due to the lack of infrastructure and scientific advancements [2]. The need for crop water requirement-based irrigation practices in these nations is high to improve irrigation efficiency. Various methods and techniques are used to estimate the crop water requirement, of which the reference evapotranspiration (ET_0) is a reliable and standard practice. ET_0 is a parameter that could be employed for all the regions based on the

local climatic parameters [3]. The estimation of models is classified as (a) fully physically-based combination models that employ mass and energy conservation principles; (b) semi-physically based models that consider either mass or energy conservation; and (3) black-box models that are empirical in nature [4,5]. Many researchers have formulated empirical and semi-empirical methods to estimate the ET_0 , like mass transfer based [6–8], radiation based [9–14], temperature based [15–17], and combination based [18,19]. Some empirical equations might require extensive agro-meteorological data, which are unavailable for every region. Therefore, there is a scope for models with less data requirement [20].

ET_0 is a phenomenon that depends on various meteorological parameters that give rise to a complex non-linear problem. Henceforth, machine learning (ML) models have been extensively used in their estimation which could solve these complex problems [21]. The previous studies available have been discussed below. Various data-driven algorithms like random forests (RF) [22–27], gradient boosting decision tree (GBDT), extreme gradient boosting (XGB) [24,27,28], light gradient boosting (LGB) [27,29–31], etc. have been employed for ET_0 estimation. Most of the research did not confine to a single algorithm. However, a comparison is made either with different machine learning techniques or empirical models. Shiri et al. [22] evaluated 12 different machine learning algorithms like multivariate adaptive regression spline (MARS), boosted regression tree (BT), random forest (RF), model tree (MT), support vector machine (SVM), etc., with other optimizers for stations in Iran using 12-year meteorological data. They have compared two input scenarios, i.e., radiation and temperature based. A study in Brazil [32] used the machine learning models like RF, XGB, artificial neural network (ANN), and convolutional neural network (CNN) models for daily and hourly ET_0 estimates. Zhou et al. [27] have used the agro-meteorological data from twelve stations in China for ET_0 prediction. They have tested the algorithms like extremely randomized trees, RF, and GBDT, and gradient boosting models like XGB, LGB, and gradient boosting with categorical features support (CatBoost), factorization machine-based neural network model (DeepFM), and SVM. They have concluded that the CatBoost and LGB models outperformed the other models, followed by XGB and GBDT.

The evaluation of ET_0 models in New Mexico, United States of America, using extreme learning machine (ELM), genetic programming (GP), RF, and SVM for different climates, was done by [33]. The results of their study indicated that the models performed in the order of SVM > ELM > RF > GP. Another study used 14 stations in different climates, i.e., arid desert, semi-arid steppe, semi-humid cold-temperate, semi-humid warm temperate, humid subtropical, and humid tropical regions in China for ET_0 prediction [30]. They have evaluated multi-layer perceptron (MLP), generalized neural network (GRNN) and adaptive neuro-fuzzy inference system (ANFIS), SVM, kernel-based non-linear extension of arps decline (KNEA), M5 model tree (M5Tree), XGB and MARS models and suggested the use of SVM over other models. Wu et al. [34] compared the basic models like RF, SVM, MLP, and K-Nearest Neighbor (KNN) regression and their stacked and blended ensemble models using data from five stations in China.

The application of different optimizers in conjunction with machine learning and deep learning models has been reported in ET_0 modelling. These research findings have revealed an improvement in accuracy over conventional ML models. Yan et al. [35] evaluated the performance of hybrid XGB coupled with whale optimization algorithm (WOA) for ET_0 modelling at humid and arid stations in China. They concluded that hybrid models had improved the accuracies in both local and external data scenarios. Grey wolf optimizer (GWO) has been employed with ANN by [36] for modelling purposes in Iran. The results were compared with least square support vector regression (LS-SVR) and conventional ANN. They found that the hybrid models were superior in their prediction. Dong et al. [37] attempted to use four types of bio-inspired optimizers with the kernel-based non-linear extension of arps decline (KNEA) model for 51 stations in China. The optimizers they employed were the grasshopper optimization algorithm (GOA), GWO, particle swarm

optimization algorithm (PSO), and salp swarm algorithm (SSA). They reported that the GWO-optimized KNEA performed better than other models.

Meta-heuristic optimizers have not been applied widely in Indian conditions, according to previous studies. Additionally, the literature lacked information on how to optimize tree-based ML models. As a result, the goal of this study is to determine if GWO can improve the efficiency of tree-based models. The specific objectives of this study are (1) to estimate the ET_0 using state-of-the-art machine learning models like RF, XGB, and LGB for humid and sub-humid climates of India; (2) to couple these models with a heuristic GWO technique for finding any improvement in the efficiency and (3) to compare various empirical models with the ML models in the study area.

2. Materials and Methods

2.1. Study Area and Data Collection

Indian climatic conditions can be broadly divided into arid, semi-arid, humid, and sub-humid regions. The humid zones over Southeast Asia have a length of growing period (LGP) of more than 270 days and an annual rainfall above 1500 mm, while the sub-humid zones have an LGP of 180 to 270 days and a rainfall amount between 1000 and 1500 mm annually [38]. The percentage of the total geographical area of sub-humid and humid regions in India is about 24% and 17%, respectively. Historically, these regions have recorded high relative humidity and adequate rainfall distribution. However, the change in bio-climates is evident due to the reduction of sub-humid and humid regions' areal extent and subsequent increase in semi-arid and arid regions over India [39]. This poses a challenge to the water availability in these regions, although with ample resources.

The agro-climatic data of sub-humid and humid regions of India were collected from the All India coordinated research project on Agro-meteorology, ICAR, from 2001 to 2020. The locations wherein the data were collected are depicted in Figure 1. The details of the stations are described in Table 1. The elevations of these stations varied from 17 m in Mohanpur to 1800 m in Ranichauri. The daily meteorological data consisting of maximum air temperature ($^{\circ}C$), minimum air temperature ($^{\circ}C$), mean relative humidity (%), wind speed at 2 m height (m/s), and the number of sunshine hours were collected from the ten locations from both the regions.

Table 1. Details of the locations of the study area.

S. No.	State	Station	Code	AER	Latitude (N)	Longitude (E)	Altitude (m)
1	Assam	Jorhat	JHT	Humid	26°45'	94°12'	116
2	West Bengal	Mohanpur	MHP	Humid	21°50'	87°15'	17
3	Himachal Pradesh	Palampur	PLP	Humid	32°07'	76°32'	1220
4	Kerala	Thrissur	TRS	Humid	10°31'	76°13'	28
5	Uttar Pradesh	Faizabad	FZB	Sub-humid	26°46'	82°08'	97
6	Madhya Pradesh	Jabalpur	JBP	Sub-humid	23°11'	79°59'	412
7	Chattisgarh	Raipur	RPR	Sub-humid	21°15'	81°37'	290
8	Jharkhand	Ranchi	RNI	Sub-humid	23°20'	85°18'	651
9	Uttarakhand	Ranichauri	RCH	Sub-humid	30°19'	78°24'	1800
10	Bihar	Samastipur	SMP	Sub-humid	25°59'	85°40'	51

These meteorological parameters affect the evapotranspiration rate by imparting the energy required for vaporization and the rate of water vapour removal from the evaporating surface. The air temperature surrounding the plant impacts the sensible heat of the air. The humidity data would affect the difference in the vapour power of the air and the evaporating surface. The wind speed affects the vapour removal, thereby affecting the evaporation rate. The sunshine data are utilized to calculate the solar radiation, which mostly affects the vaporization of the water to vapour.

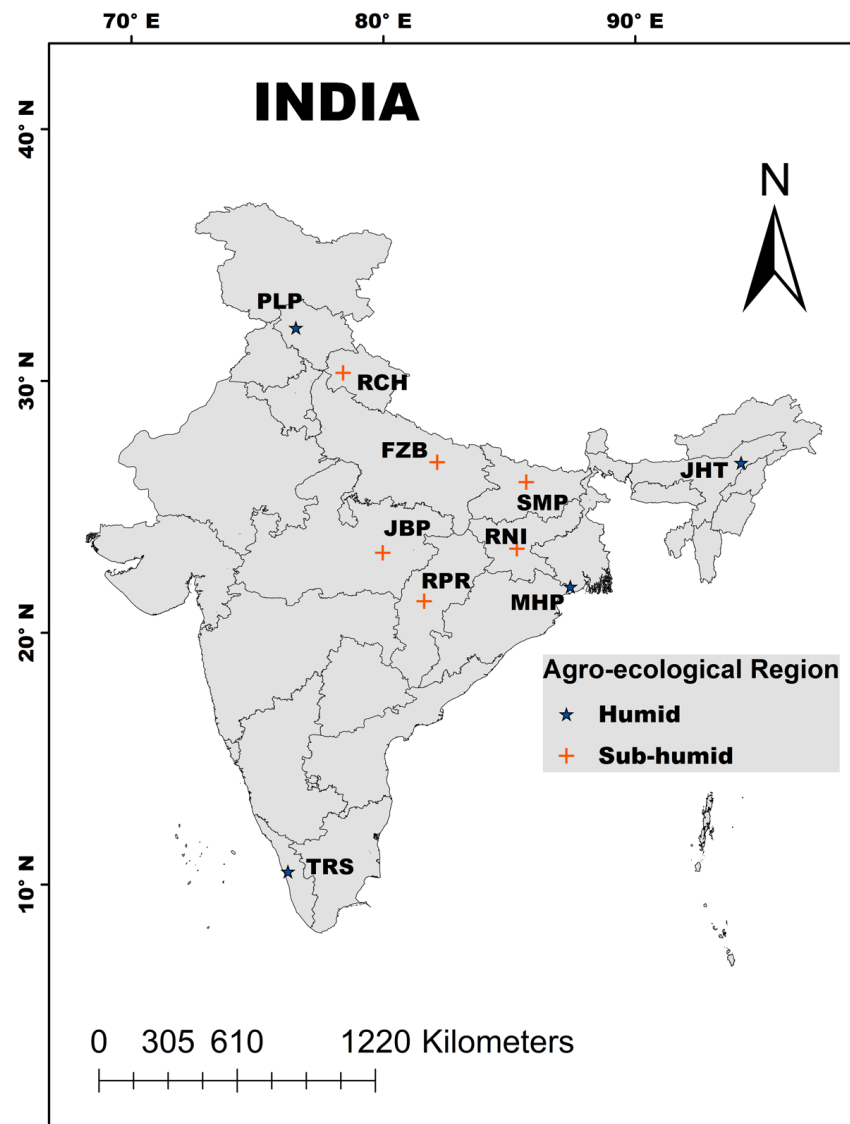


Figure 1. Study area map showing locations in humid and sub-humid regions.

2.2. ET_0 Estimation Using FAO-56 Penman-Monteith and Empirical Equations

The ASCE Committee on Irrigation and Water requirements analysed different methods in estimating ET_0 . They found that the FAO 56 Penman-Monteith can be used in all locations. Hence, the standardised equation of reference evapotranspiration is used as the target variable in the modelling stages. The equation for predicting ET_0 by FAO 56 Penman-Monteith is given below. The machine learning models were compared with different empirical equations. The estimation of ET_0 using different empirical equations using the formulae as described in Table 2.

Table 2. Formulae for FAO 56 Penman-Monteith and empirical equations used.

Method	Symbol and Equations	Reference
Target for the Models		
FAO-56 Penman-Monteith	$ET_{PM} = \frac{0.408\Delta(R_n - G) + \gamma \frac{900}{T_{mean} + 273} u_2 (e_s - e_a)}{\Delta + \gamma(1 + 0.34 u_2)}$	(1) [40]
Mass Transfer based		
Albrecht (ALB)	$ET_{ALB} = F (e_s - e_a)$ where $F = 0.4$ if $u_2 \geq 1$ m/s and $F = 0.1005 + 0.297 u_2$, if $u_2 < 1$ m/s	(2) [6]
Mahringer (MAH)	$ET_{MAH} = 0.15072 \sqrt{3.6 u_2} (e_s - e_a),$ where $(e_s - e_a)$ in hPa	(3) [7]
Penman (PEN)	$ET_{PEN} = 0.35 \left(1 + \frac{0.98}{100 u_2}\right) (e_s - e_a),$ where $(e_s - e_a)$ in mm Hg and u_2 in miles per day	(4) [8,41]
Radiation based		
Jensen-Haise (JH)	$ET_{JH} = \left(\frac{R_s}{\lambda}\right) (0.025 T_{mean} + 0.08)$	(5) [11,42]
Makkink (MAK)	$ET_{MAK} = 0.61 \left(\frac{\Delta}{\Delta + \gamma}\right) \left(\frac{R_s}{\lambda}\right) - 0.12$	(6) [43]
McGuinness-Bordne (MGB)	$ET_{MGB} = \left(\frac{R_a}{\lambda \rho}\right) \left(\frac{T_{mean} + 5}{68}\right)$	(7) [12]
Priestly-Taylor (PT)	$ET_{PT} = 1.26 \left(\frac{\Delta}{\Delta + \gamma}\right) \left(\frac{R_n}{\lambda}\right)$	(8) [13]
Turc (TUR)	$ET_{TUR} = 0.013 \left(\frac{T_{mean}}{T_{mean} + 15}\right) (23.8846 R_s + 50), \text{ for } RH > 50\% = 0.013 \left(\frac{T_{mean}}{T_{mean} + 15}\right) (23.8846 R_s + 50) \left(1 + \frac{50 - RH}{70}\right), \text{ for } RH < 50\%$	(9) [14]
Temperature based		
Hargreaves-Samani (HS)	$ET_{H-S} = 0.0026 \sqrt{T_{max} - T_{min}} (T_{mean} + 17.8) (0.408 R_a)$	(10) [16]
Hargreaves-Samani 1 (HS1)	$ET_{HS1} = 0.0030 (T_{max} - T_{min})^{0.4} (T_{mean} + 20) (0.408 R_a)$	(11) [17]
Hargreaves-Samani 2 (HS2)	$ET_{HS2} = 0.0025 \sqrt{T_{max} - T_{min}} (T_{mean} + 16.8) (0.408 R_a)$	(12) [17]
Thorthwaite (Modified) (THO)	$ET_{THO} = 0.533 \frac{N}{12} \left(\frac{10 T_{mean}}{33.617}\right)^{1.033}$	(13) [44]
Combination based		
Copais (COP)	$ET_{COP} = 0.057 + 0.277(-0.0033 + 0.00812 T_{mean} + 0.101 R_s + 0.00584 R_s T_{mean}) + 0.643 (0.6416 - 0.00784 RH + 0.372 R_s - 0.00364 RH) + 0.0124 (0.6416 - 0.00784 RH + 0.372 R_s - 0.00364 RH)(-0.0033 + 0.00812 T_{mean} + 0.101 R_s + 0.00584 R_s T_{mean})$	(14) [18]
Valiantzas 1 (VA1)	$ET_{VA1} = 0.0393 R_s \sqrt{T_{mean} + 9.5} - 0.19 R_s^{0.6} \varphi^{0.15} + 0.078 (T_{mean} + 20) \left(1 - \frac{RH}{100}\right)$	(15) [19]
Valiantzas 2 (VA2)	$ET_{VA2} = 0.0393 R_s \sqrt{T_{mean} + 9.5} - 0.19 R_s^{0.6} \varphi^{0.15} + 0.0061 (T_{mean} + 20) (1.12 T_{mean} - T_{min} - 2)^{0.7}$	(16) [19]

Notes: Units and Description of the parameters unless specified above: ET is the reference evapotranspiration, mm/day; Δ is the slope of the vapour pressure curve, kPa/°C, R_n is the net radiation at the crop surface in MJ/ m² day, G is the soil heat flux density in MJ/ m² day, γ is the psychrometric constant in kPa/°C, e_s is the saturation vapour pressure, kPa; e_a is the actual vapour pressure, kPa; u_2 is the wind speed at 2 m above the ground surface, m/s; T_{mean} is the mean daily air temperature, °C; R_n is the net solar radiation, MJ/m² day; R_s is the incident shortwave solar radiation flux, MJ/m²/day; R_a is the extra-terrestrial solar radiation, MJ/m² day; T_{max} is the maximum daily air temperature, °C; T_{min} is the minimum daily air temperature, °C; N is the maximum possible duration, hrs; RH is the mean daily relative humidity, %; and φ is latitude, Radians.

2.3. Description of Machine Learning Models and Optimizer

2.3.1. Random Forest (RF)

RF model generates output predictions by combining results from several regression decision trees. RF is capable of capturing complex, non-linear interactions between the features and produces a powerful prediction model. Being an ensemble method, RF trains several decision trees in parallel with bootstrapping followed by aggregation (Figure 2a). The trees in the ‘forest’ are generated based on a random selection of subset data from the training set, and the bootstrapping ensures that each tree in the forest is unique [45,46]. For the final prediction, the RF regressor aggregates the decision made by individual

trees. RF is robust to outliers, produces better generalization, and has easily tunable hyperparameters [47].

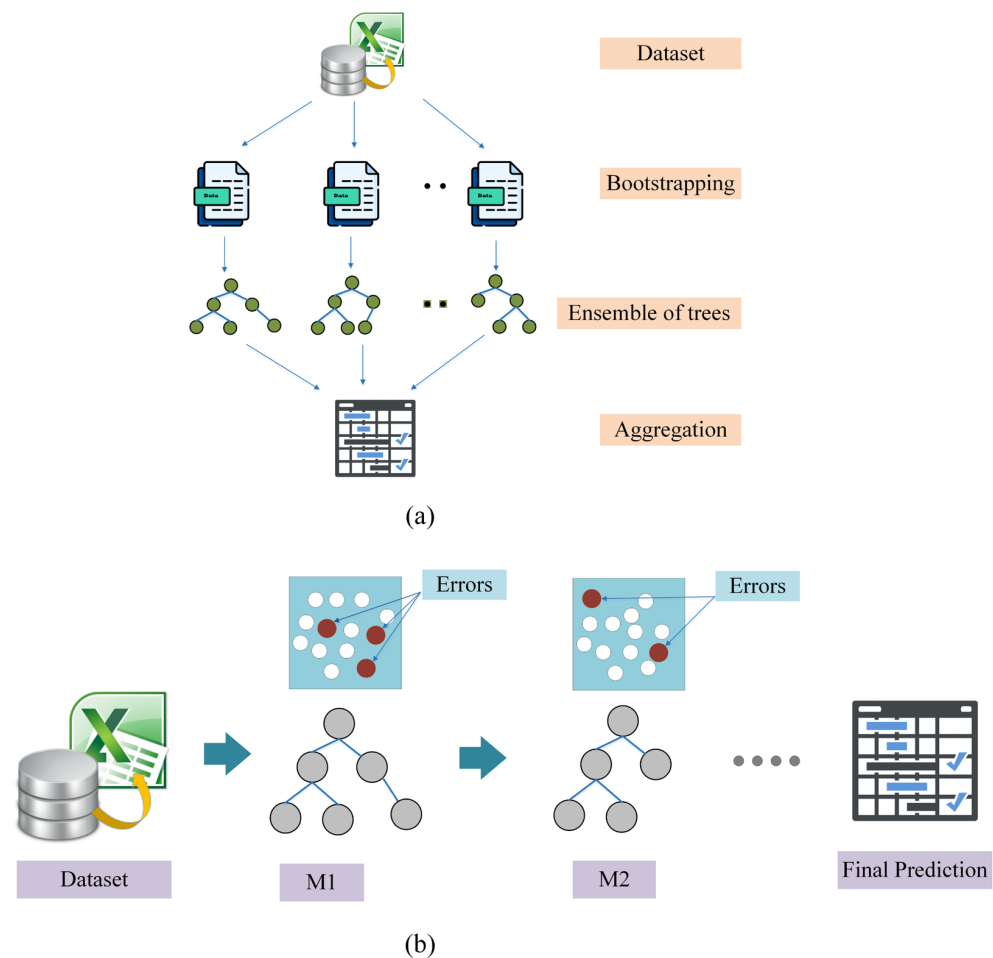


Figure 2. Data flow in (a) bagging (RF) and (b) boosting (XGB/LGB) models.

2.3.2. Extreme Gradient Boosting Model (XGB)

XGB provides an efficient and scalable implementation of gradient boosting framework [48] suitable for both regression and classification problems. A typical gradient-boosting approach is an ensemble of decision trees that are trained in a sequential manner [49]. In gradient boosting, a better model is built by merging previous models until the best model reduces the cumulative prediction error (Figure 2b). XGB was developed with optimized and supports distributed computing, additionally improving flexibility and portability. XGB leverages parallel computation to build trees across different processing units. The algorithm supports effective pruning of trees for improving the computational speed and sparsity-aware split finding to handle the missing data.

2.3.3. Light Gradient Boosting Model (LGB)

The LGB model is a gradient-boosting framework built on decision trees that boosts the model's effectiveness and consumes less memory. The key characteristic of LGB is that the trees are grown leaf-wise instead of checking all of the previous leaves for each new leaf [50]. LGB uses two novel approaches, viz., Gradient-based One Side Sampling and Exclusive Feature Bundling (EFB), to achieve improved performance. Using the GOSS, the major portion of the data points with small gradients are eliminated from calculating the information gain, achieving significant time saving [51]. Using EFB, the mutually exclusive features are bundled, achieving feature reduction without compromising the

model performance. The model works effectively on benchmark datasets with increased training speed compared to the conventional gradient-boosting methods.

2.3.4. Grey Wolf Optimizer (GWO)

GWO is an evolutionary, meta-heuristic algorithm inspired by the structure of the leadership hierarchy and hunting mechanism of grey wolves in nature [52] and has been proven to be a more practical and precise method for optimization problems [53]. It has significant advantages over the other swarm intelligence approaches, such as a reduced number of parameters and no requirement of derivation information during the initial search, etc. [54]. In GWO, a grey wolf herd's members are classified as α , β , δ and ω and depending on the effectiveness, decision-making ability, and way of advancing in the hunting process.

The α wolves are the strongest and most powerful, usually serves as the herd's leader and should be obeyed by the other wolves in the pack. β wolves act as advisors to the alpha group, and δ wolves act in the group as guards, sentinels, and hunters. The ω group of wolves is in the lowest position of decision-making [55] and follows others. The alpha in GWO is believed to be the best answer. In order of priority, the beta, gamma, and omega solutions come next. The wolves in GWO iterations assess the potential for a hunt and adjust their status accordingly (Figure 3).

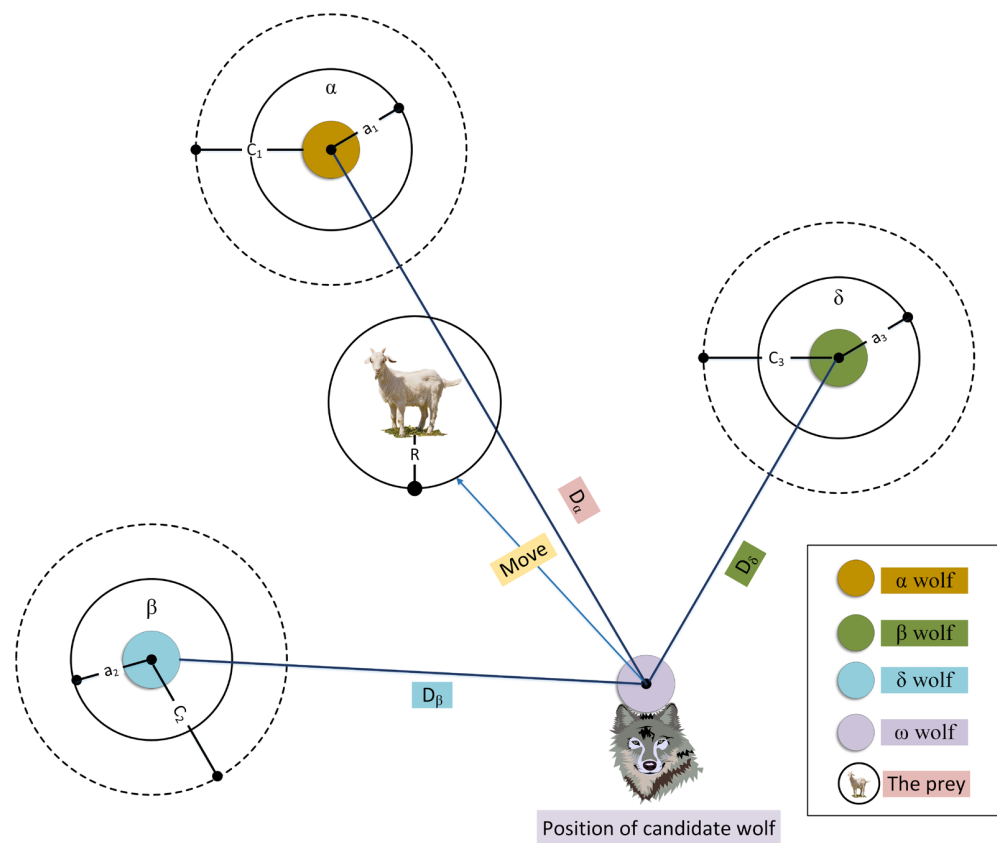


Figure 3. Schematic diagram of GWO optimizers (Source: [56]).

2.4. ET_0 Estimator Using ML and Hybrid ML

2.4.1. Input Scenarios

The daily meteorological parameters from 2001 to 2020 at all ten stations are used as the inputs for the modelling of daily ET_0 . The inputs consisted of maximum air temperature (T_{max} , °C), minimum air temperature (T_{min} , °C), mean relative humidity (RH, %), wind speed at 2 m height (u_2 , m/s), number of sunshine hours (n, hours), solar radiation (R_n , MJ/m² day) and extra-terrestrial radiation (R_a , MJ/m² day).

A total of 18 combinations were employed. Table 3 depicts the different combinations used, ranging from two inputs in model index 1 to six inputs in model indices 17 and 18. The target for these models was the daily ET_0 calculated from the FAO-56 Penman-Monteith equation. The statistical indicators of the inputs and output at various stations are presented in Figure S1. The time series graphs of ET_0 from some stations of the study on a daily basis from 2001 to 2020 were shown in Figure S2 (Supplementary Materials).

Table 3. Data input scenarios.

Model Index	Input Combinations	Model Index	Input Combinations
1	T_{max}, T_{min}	10	$T_{max}, T_{min}, RH, R_a$
2	T_{max}, T_{min}, RH	11	$T_{max}, T_{min}, U_2, R_a$
3	T_{max}, T_{min}, U_2	12	T_{max}, T_{min}, n, R_a
4	T_{max}, T_{min}, n	13	$T_{max}, T_{min}, RH, U_2$
5	T_{max}, T_{min}, R_s	14	T_{max}, T_{min}, RH, n
6	T_{max}, T_{min}, R_a	15	T_{max}, T_{min}, U_2, n
7	$T_{max}, T_{min}, RH, R_s$	16	$T_{max}, T_{min}, RH, U_2, n$
8	$T_{max}, T_{min}, U_2, R_s$	17	$T_{max}, T_{min}, RH, U_2, n, R_s$
9	T_{max}, T_{min}, n, R_s	18	$T_{max}, T_{min}, RH, U_2, n, R_a$

2.4.2. Model Development

The data were normalised, which gives scale uniformity, improving the modelling capability. The normalised input data were used for modelling purposes [57]. The equation used for the normalisation of the data is given below:

$$x_{norm} = \frac{x_0 - x_{min}}{x_{max} - x_{min}} \quad (17)$$

where: x_{norm} is the normalised value of the input, x_0 is the actual value of the input that is being normalised, and x_{max} and x_{min} are the maximum and minimum values of all the inputs.

Fivefold cross-validation was employed in each of the ML and hybrid ML models, as shown in Table 4. For example, say in the V1 scenario, 16-year daily data from 2005 to 2020 would be used for the model training, and the rest of the data from 2001 to 2004 would be used for the testing of the model developed. This was done for the rest of the cross-validation stages as well so that the whole of the data set would be tested for accuracy. The employment of cross-validation has been found to reduce the over-fitting of the models [24].

Table 4. Cross-validation stages.

Cross-Validation	Training	Testing
V1	2005–2020	2001–2004
V2	2001–2004 and 2009–2020	2005–2008
V3	2001–2008 and 2013–2020	2009–2012
V4	2001–2012 and 2017–2020	2013–2016
V5	2001–2016	2017–2020

2.4.3. Hyper Parameter Tuning in Hybrid ML

The hybrid ML models were developed by optimization of the hyperparameters of RF, XGB, and LGB models using the GWO algorithm. The default values and the range of hyperparameters used in the study are shown in Table 5. The default values of the hyperparameters were used in the state-of-the-art ML models, whereas the best hyperparameter set in each of the ML models was assessed using the GWO to develop the hybrid models, i.e., GWORF, GWOXGB, and GWOLGB. The fine-tuning of hyperparameters could potentially improve the prediction accuracy of hybrid models [58].

Table 5. Hyperparameter plane for tuning the parameters using GWO.

Model	Parameter	Default Value	Hyperparameter Range for Tuning
RF	n_estimators	100	Range of 10 to 500, increment by 10
	min_samples_leaf	1	Range of 1 to 6, increment by 2
	max_depth	None	Range of 2 to 20, increment by 2 and None
XGB	n_estimators	100	Range of 10 to 500, increment by 10
	learning_rate	0.3	[0.05, 0.1, 0.15, 0.3]
	max_depth	6	Range of 2 to 20, increment by 2 and None
LGB	n_estimators	100	Range of 10 to 500, increment by 10
	learning_rate	0.3	[0.05, 0.1, 0.15, 0.3]
	max_depth	6	Range of 2 to 20, increment by 2 and None

2.5. Model Performance Indicators

The indicators used in the study were root mean square error (RMSE), coefficient of determination (R^2), mean absolute error (MAE) [27], and agreement index (d) [59]. The formulae for these indicators are described in Table 6.

Table 6. Statistical indicators.

Indicator	Code	Formula
Root mean square error	RMSE	$\sqrt{\frac{\sum_{i=1}^N (O_i - P_i)^2}{N}}$ (18)
Coefficient of determination	R^2	$\left(\frac{\sum_{i=1}^N \{ (O_i - \bar{O}_i)(P_i - \bar{P}_i) \}}{\sqrt{\sum_{i=1}^N (O_i - \bar{O}_i)^2 \sum_{i=1}^N (P_i - \bar{P}_i)^2}} \right)^2$ (19)
Mean absolute error	MAE	$\frac{\sum_{i=1}^N P_i - O_i }{N}$ (20)
Agreement index	d	$1 - \frac{\sum_{i=1}^N (P_i - O_i)^2}{\sum_{i=1}^N (P_i - \bar{O}_i + O_i - \bar{O}_i)^2}$ (21)

Notes: N is the total number of test data, O_i and P_i are the actual ET_0 by FAO 56 Penman-Monteith and predicted values of the models, respectively.

Global Performance Indicator (GPI)

Using different indicators renders a problem in properly selecting or judging the best models. Hence, a summative index that uses the equation called Global Performance Indicator is used in the study [36]. All the above indicators, i.e., RMSE, R^2 , MAE, d, were normalized between 0 and 1 using Equation (22), and the value of GPI for a model is found using Equation (23). Higher values of GPI would give the best model compared to other models [60,61].

$$N_j = \frac{S_j - \min(S)}{\max(S) - \min(S)} \tag{22}$$

N_j is the normalized statistical index, S_j is the original statistical index, $\min(S)$ is the minimum value in that statistical index, and $\max(S)$ is the maximum value in that statistical index.

$$GPI_i = \sum_{j=1}^n (S_j - S_{ij}) \alpha_j \tag{23}$$

GPI_i is the value of the Global Performance Indicator for model i , S_j is the median value of the statistical indicator j , S_{ij} is the value of the statistical indicator j for model i , α_j is a constant with a value of -1 for R^2 , d and 1 for MAE, RMSE. The ranking based on the GPI value was also done.

3. Results

3.1. Comparison of the Empirical Models in Estimating ET_0

Evaluation of different empirical models was carried out against the FAO-56 Penman-Method as the target for the daily data of 20 years at both humid and sub-humid locations.

The performance indicators of the fifteen models at humid and sub-humid stations were presented in Tables S1 and S2, respectively. The ranking of the various models at humid stations based on the GPI is depicted in Table 7. The comparison at various stations suggests that the radiation-based models were superior at most stations. In contrast, mass-transfer-based models were found to be of low accuracy. It shows that the Turc Model was a promising method compared to other models. It was followed by Makkink, Valiantzas 2, Jensen-Haise. The lowest-performing empirical models in the humid region were McGuinness-Bordne, Mahringer, and Valiantzas 1. The ranking of the various models at sub-humid stations is shown in Table 8. The superior models in sub-humid regions were Turc, Valiantzas 2, Jensen-Haise, and Priestly-Taylor. The worst empirical models at sub-humid stations were Valiantzas 1, Albrecht, Copias, and Mahringer. The results indicated that the empirical model performance varied at different stations. Overall, the Turc model could be used in the study area based on its superior ranking in most stations.

Table 7. Ranking of the best-performing empirical models at humid stations.

RANK	Jorhat		Mohanpur		Palampur		Thrissur	
	MODEL	GPI	MODEL	GPI	MODEL	GPI	MODEL	GPI
1	TUR	1.467	MAK	1.521	TUR	1.423	TUR	1.439
2	PT	1.390	TUR	1.508	VA2	1.292	VA2	1.305
3	MAK	1.276	PT	1.330	JH	0.863	PT	0.818
4	VA2	1.216	VA2	1.027	HS	0.783	MAK	0.769
5	JH	0.550	VA1	0.813	PT	0.721	PEN	0.372
6	VA1	0.484	HS	0.361	HS2	0.663	JH	0.154
7	HS	-0.265	HS2	0.082	MAK	0.613	ALB	0.034
8	ALB	-0.302	HS1	0.052	HS1	0.467	HS	0.028
9	COP	-0.370	THO	0.032	THO	-0.233	MAH	-0.084
10	HS2	-0.488	JH	-0.092	MAH	-0.516	HS2	-0.111
11	HS1	-0.552	COP	-0.812	PEN	-0.517	COP	-0.171
12	THO	-0.579	ALB	-1.033	ALB	-0.586	HS1	-0.351
13	PEN	-0.782	PEN	-1.173	COP	-1.071	VA1	-0.727
14	MAH	-0.807	MAH	-1.687	MGB	-1.323	THO	-0.917
15	MGB	-2.238	MGB	-1.927	VA1	-2.577	MGB	-2.559

Table 8. Ranking of the best-performing empirical models at sub-humid stations.

RANK	Faizabad		Jabalpur		Raipur		Ranchi		Ranichauri		Samastipur	
	MODEL	GPI	MODEL	GPI	MODEL	GPI	MODEL	GPI	MODEL	GPI	MODEL	GPI
1	TUR	1.037	TUR	1.234	TUR	1.117	TUR	1.587	VA2	1.487	TUR	1.037
2	JH	0.882	VA2	1.014	VA2	0.969	PT	1.510	TUR	1.468	JH	0.882
3	VA2	0.840	PT	0.887	HS	0.894	VA2	1.294	MAK	1.258	VA2	0.840
4	HS	0.642	HS	0.686	PT	0.784	MAK	1.122	JH	1.048	HS	0.642
5	HS1	0.520	JH	0.646	HS1	0.722	JH	0.347	PT	0.932	HS1	0.520
6	PT	0.517	HS1	0.487	HS2	0.705	HS	0.311	HS	0.875	PT	0.517
7	HS2	0.500	THO	0.444	JH	0.556	THO	0.262	HS2	0.762	HS2	0.500
8	THO	0.390	HS2	0.440	THO	0.414	HS1	-0.059	HS1	0.544	THO	0.390
9	COP	0.119	MAK	0.377	MAK	0.171	HS2	-0.065	THO	-0.279	COP	0.119
10	PEN	0.050	PEN	-0.150	PEN	-0.131	ALB	-0.643	ALB	-1.032	PEN	0.050
11	MAK	-0.007	COP	-0.554	COP	-0.386	PEN	-0.661	MGB	-1.038	MAK	-0.007
12	MGB	-0.737	MAH	-0.883	MAH	-1.053	MAH	-0.729	MAH	-1.230	MGB	-0.737
13	MAH	-1.148	MGB	-1.016	MGB	-1.106	VA1	-0.744	VA1	-1.552	MAH	-1.148
14	ALB	-1.212	ALB	-1.501	ALB	-1.523	COP	-1.493	COP	-1.567	ALB	-1.212
15	VA1	-2.392	VA1	-2.110	VA1	-2.131	MGB	-2.041	PEN	-1.675	VA1	-2.392

3.2. Comparison of Various Input Combinations in Conventional ML Models

3.2.1. Best-Performing Models in ML

The three conventional models used in the study, i.e., RF, XGB, and LGB, were evaluated with various input combinations. The results in these sections are for the testing data sets in all the cross-validation stages. The statistical indicators at each station using the conventional ML models are given in Tables S3–S12. It was observed that the R^2 value has improved with higher inputs, and LGB models were more accurate than other models. A substantial increase in the accuracy and reduced errors was observed in model indices 8 and 9 across all the stations. The ranking of the eighteen best models (six models in each ML) at humid locations based on the GPI is shown in Table 9. The results indicated that the models that used the most inputs (Index 17 and 18) were superior with higher GPI. The LGB17 and LGB18 performed best in Palampur and Thrissur, whereas the XGB17 was the best at Jorhat and Mohanpur. It was observed that the XGB8 and LGB8, which used wind speed and solar radiation data, performed better in all the stations except Palampur, where the LGB7, RF7, and XGB7 gave accurate estimates. Overall, the performance of RF was found to be inferior to both XGB and LGB. The lowest error (RMSE = 0.096 mm/day) was found using XGB17 at Mohanpur station and, the highest R^2 value (0.994) was observed at Palampur and Thrissur for LGB18 and at Mohanpur for LGB17.

Table 9. Ranking of the best-performing ML models at humid stations.

RANK	Jorhat		Mohanpur		Palampur		Thrissur	
	MODEL	GPI	MODEL	GPI	MODEL	GPI	MODEL	GPI
1	XGB17	1.889	XGB17	1.941	LGB18	1.952	LGB18	1.199
2	XGB18	1.753	LGB17	1.939	LGB17	1.893	LGB17	1.187
3	LGB17	1.717	LGB18	1.721	XGB18	1.777	XGB17	1.159
4	LGB18	1.716	XGB18	1.691	XGB17	1.755	XGB18	1.118
5	RF17	0.795	RF17	1.424	RF18	1.658	RF17	0.911
6	XGB8	0.748	RF18	1.286	RF17	1.501	RF18	0.769
7	LGB8	0.721	LGB8	0.853	LGB7	−0.063	LGB16	0.224
8	RF18	0.582	XGB8	0.702	RF7	−0.146	LGB8	0.130
9	RF8	0.309	RF9	0.607	XGB7	−0.258	XGB16	0.077
10	RF9	0.304	RF8	0.598	LGB16	−0.337	XGB8	0.067
11	LGB12	−0.699	LGB9	−1.208	RF16	−0.527	RF16	−0.008
12	LGB9	−0.726	LGB12	−1.369	XGB16	−0.628	RF8	−0.010
13	RF12	−1.040	RF12	−1.439	LGB8	−1.070	RF9	−0.017
14	XGB9	−1.231	LGB7	−1.546	RF8	−1.191	LGB15	−0.413
15	XGB12	−1.321	XGB9	−1.619	RF9	−1.212	RF15	−0.536
16	LGB7	−1.633	RF7	−1.712	XGB8	−1.373	XGB15	−0.558
17	RF7	−1.806	XGB12	−1.815	LGB12	−1.684	LGB7	−2.499
18	XGB7	−2.079	XGB7	−2.053	XGB12	−2.048	XGB7	−2.801

The eighteen best-ranking models at sub-humid locations are shown in Table 10. It could be seen that the LGB17 and LGB18 were the best performing at all the six stations. The performance of the model indices 8, 9, and 16 was quite promising at all the stations except at Ranichauri, wherein the index 7 models were accurate. It was observed that the addition of solar radiation as an input considerably increased the performance of the models. The models that correlated with the FAO-56 Penman-Monteith are in the order of LGB, XGB, and RF. The LGB18 at Jabalpur station performed well ($R^2 = 0.995$), whereas the least RMSE (0.094 mm/day) was recorded at Ranichauri for LGB17.

Table 10. Ranking of the best-performing ML models at sub-humid stations.

RANK	Faizabad		Jabalpur		Raipur		Ranchi		Ranichauri		Samastipur	
	MODEL	GPI	MODEL	GPI	MODEL	GPI	MODEL	GPI	MODEL	GPI	MODEL	GPI
1	LGB17	1.752	LGB18	1.265	LGB18	1.265	LGB17	1.637	LGB17	2.374	LGB17	1.908
2	LGB18	1.682	LGB17	1.222	LGB17	1.248	XGB17	1.593	LGB18	2.303	LGB18	1.821
3	XGB17	1.630	XGB18	1.138	XGB18	1.197	LGB18	1.566	XGB17	2.207	XGB17	1.761
4	XGB18	1.561	XGB17	1.137	XGB17	1.191	XGB18	1.546	XGB18	2.034	XGB18	1.583
5	RF17	1.373	RF17	0.993	RF17	1.036	RF17	1.147	RF18	1.693	RF17	1.397
6	RF18	1.321	RF18	0.965	RF18	0.973	RF18	1.065	RF17	1.531	RF18	1.041
7	LGB16	0.162	LGB16	0.347	LGB16	0.473	LGB8	0.463	LGB7	0.216	LGB8	0.282
8	XGB16	−0.027	XGB16	0.195	XGB16	0.323	RF8	0.321	RF7	−0.005	RF9	0.135
9	LGB8	−0.125	RF16	0.112	RF16	0.247	RF9	0.304	XGB7	−0.071	RF8	0.128
10	RF9	−0.156	LGB8	0.079	LGB8	−0.070	XGB8	0.281	LGB9	−1.159	XGB8	0.037
11	RF8	−0.195	RF8	0.016	RF9	−0.131	LGB16	−0.394	LGB8	−1.164	LGB16	−0.586
12	RF16	−0.289	RF9	0.015	RF8	−0.140	XGB16	−0.601	LGB12	−1.237	RF16	−0.746
13	XGB8	−0.298	XGB8	−0.076	XGB8	−0.193	RF16	−0.749	RF9	−1.358	XGB16	−0.888
14	LGB15	−1.194	LGB15	−0.608	LGB15	−0.607	LGB15	−1.136	RF8	−1.388	LGB7	−1.211
15	XGB15	−1.460	RF15	−0.769	RF15	−0.771	RF15	−1.357	RF12	−1.416	RF7	−1.354
16	RF15	−1.520	XGB15	−0.845	XGB15	−0.851	XGB15	−1.361	XGB9	−1.459	XGB7	−1.502
17	LGB13	−1.970	LGB13	−2.450	LGB13	−2.455	LGB12	−1.962	XGB8	−1.474	LGB15	−1.713
18	XGB13	−2.248	XGB13	−2.735	XGB13	−2.735	XGB12	−2.363	XGB12	−1.626	XGB12	−2.092

3.2.2. Least-Performing Models in ML

The ranking of the low-performing models at humid locations of all the conventional model and their input combinations are shown in Table 11. The results showed that model indices 1, 2, 3, and 6 were the least ranked models. It was obvious that the model that used the least number of inputs (only temperature data) was the worst model in estimating ET₀. The RF models had the lowest GPI values compared to other models' counterparts at most stations, indicating their higher errors. It was observed that the LGB models performed better than other ML models using the same input combinations. The error was found to be highest (RMSE = 0.919 mm/day) at Thrissur using RF1, whereas the least R² (0.371) was seen at Jorhat for RF1. The model combination that used extra-terrestrial radiation, i.e., model indices 10 and 11, did not yield accurate results.

Table 11. Ranking of the least-performing ML models at humid stations.

RANK	Jorhat		Mohanpur		Palampur		Thrissur	
	MODEL	GPI	MODEL	GPI	MODEL	GPI	MODEL	GPI
54	RF1	−2.139	RF1	−2.503	RF1	−2.748	RF1	−2.429
53	XGB1	−1.541	XGB1	−1.401	XGB1	−2.185	XGB1	−1.862
52	LGB1	−1.099	RF2	−1.098	LGB1	−1.766	LGB1	−1.542
51	RF3	−0.885	XGB2	−0.907	RF3	−0.781	RF6	−1.450
50	XGB3	−0.743	LGB1	−0.789	XGB3	−0.390	XGB6	−1.296
49	XGB6	−0.458	RF3	−0.404	RF6	−0.249	LGB6	−1.054
48	LGB3	−0.405	LGB2	−0.208	XGB6	−0.071	RF2	−0.006
47	RF6	−0.403	XGB3	−0.142	LGB3	−0.042	XGB2	0.111
46	XGB11	−0.036	RF6	0.032	LGB6	0.410	XGB10	0.332
45	RF11	−0.028	XGB6	0.117	RF4	0.497	LGB2	0.334
44	LGB6	0.029	XGB13	0.513	RF2	0.607	RF10	0.362
43	LGB11	0.198	LGB3	0.533	XGB4	0.704	LGB10	0.569
42	RF2	0.649	RF13	0.728	XGB11	0.733	RF3	1.111
41	XGB2	0.682	LGB6	0.813	XGB2	0.807	XGB3	1.130
40	LGB2	1.076	XGB10	0.884	RF11	0.976	LGB3	1.335
39	XGB10	1.532	RF10	1.141	LGB4	1.110	XGB13	1.372
38	RF10	1.709	LGB13	1.192	LGB11	1.190	RF5	1.413
37	LGB10	1.861	LGB10	1.497	LGB2	1.197	LGB5	1.571

The results at the sub-humid stations were found to be quite similar to that of humid locations (Table 12). The model indices 1, 2, 6, and 3 were ranked the lowest in most stations.

The highest RMSE of 1.253 mm/day was observed at Faizabad station using the RF1 model, whereas the lowest R^2 (0.631) was reported at Samastipur with the same set of ML model.

Table 12. Ranking of the least-performing ML models at sub-humid stations.

RANK	Faizabad		Jabalpur		Raipur		Ranchi		Ranichauri		Samastipur	
	MODEL	GPI	MODEL	GPI	MODEL	GPI	MODEL	GPI	MODEL	GPI	MODEL	GPI
54	RF1	-2.377	RF1	-2.344	RF1	-2.271	RF1	-2.028	RF1	-2.560	RF1	-2.505
53	XGB1	-1.815	XGB1	-1.787	XGB1	-1.686	XGB2	-1.328	XGB1	-1.774	XGB1	-1.999
52	LGB1	-0.991	LGB1	-1.128	LGB1	-0.998	RF2	-1.215	LGB1	-1.307	LGB1	-1.514
51	XGB2	-0.618	XGB2	-1.103	XGB2	-0.758	XGB1	-1.164	RF3	-1.065	RF6	-0.654
50	RF2	-0.471	RF2	-0.919	RF2	-0.629	LGB2	-0.549	XGB3	-1.047	XGB6	-0.624
49	RF6	-0.439	XGB6	-0.504	XGB6	-0.544	LGB1	-0.509	LGB3	-0.596	XGB2	-0.315
48	XGB4	-0.407	LGB2	-0.475	RF6	-0.524	XGB10	-0.480	XGB2	-0.131	RF2	-0.202
47	XGB6	-0.388	RF6	-0.283	LGB2	-0.302	XGB6	-0.419	RF2	-0.075	LGB6	-0.161
46	RF4	-0.171	LGB6	0.106	XGB10	-0.096	RF6	-0.268	LGB2	0.287	XGB3	0.053
45	LGB2	-0.021	XGB10	0.132	LGB6	0.072	RF10	-0.097	XGB6	0.497	LGB2	0.172
44	LGB6	0.068	RF10	0.479	RF10	0.333	LGB10	0.354	RF6	0.560	RF3	0.224
43	LGB4	0.357	LGB10	0.601	XGB4	0.449	LGB6	0.419	XGB13	0.641	LGB3	0.523
42	XGB14	0.792	XGB4	0.842	LGB10	0.615	XGB3	0.629	RF13	0.790	XGB11	0.790
41	RF14	1.069	RF4	0.912	RF4	0.713	RF3	0.677	LGB6	0.843	RF11	1.055
40	XGB10	1.185	LGB4	1.255	LGB4	1.088	XGB13	1.228	LGB13	1.026	XGB10	1.115
39	LGB14	1.263	XGB3	1.277	XGB5	1.178	LGB3	1.306	XGB11	1.104	LGB11	1.232
38	RF5	1.339	RF3	1.285	RF5	1.632	RF13	1.473	RF11	1.366	RF10	1.316
37	LGB10	1.623	LGB14	1.656	LGB14	1.729	LGB13	1.972	LGB11	1.440	LGB10	1.495

3.3. Empirical Models v/s Conventional ML Models

The conventional ML models were compared with the empirical equations that employed a similar combination of inputs for modelling. The results at humid (Table 13) and sub-humid locations (Table 14) depicted that the ML models outperformed the empirical models with high GPI values at all combinations and locations. It could be observed that in indices 13, 5, 6, and 7, the models performed in the order of LGB, RF, and XGB.

Table 13. Comparison of the empirical models with conventional ML models (Humid).

Inputs used	Jorhat		Mohanpur		Palampur		Thrissur		
	RANK	MODEL	GPI	MODEL	GPI	MODEL	GPI	MODEL	GPI
$T_{max}, T_{min}, RH, U_2$	1	LGB13	1.708	LGB13	1.696	LGB13	1.908	LGB13	1.802
	2	RF13	1.576	RF13	1.639	RF13	1.844	RF13	1.690
	3	XGB13	1.561	XGB13	1.612	XGB13	1.808	XGB13	1.639
	4	ALB	-0.988	ALB	-1.315	MAH	-1.786	PEN	-1.195
	5	PEN	-1.823	PEN	-1.501	PEN	-1.849	ALB	-1.842
	6	MAH	-2.034	MAH	-2.132	ALB	-1.925	MAH	-2.093
T_{max}, T_{min}, R_s	1	LGB5	0.824	LGB5	0.982	LGB5	1.037	LGB5	0.942
	2	RF5	0.792	RF5	0.974	XGB5	0.990	RF5	0.907
	3	XGB5	0.786	XGB5	0.966	RF5	0.975	XGB5	0.902
	4	PT	0.560	MAK	0.501	JH	0.178	PT	0.337
	5	MAK	0.410	PT	0.435	PT	-0.001	MAK	0.293
	6	JH	-0.246	JH	-0.870	MAK	-0.216	JH	-0.323
	7	MGB	-3.126	MGB	-2.988	MGB	-2.963	MGB	-3.058
T_{max}, T_{min}, R_a	1	LGB6	2.110	LGB6	1.864	LGB6	1.306	LGB6	1.678
	2	RF6	1.483	XGB6	1.660	XGB6	1.071	XGB6	1.525
	3	XGB6	1.369	RF6	1.635	RF6	0.984	RF6	1.436
	4	HS	-0.676	HS	-0.685	HS	0.352	HS	-0.212
	5	HS1	-1.245	HS2	-1.400	HS2	-0.163	HS2	-0.746
	6	HS2	-1.328	HS1	-1.416	HS1	-0.856	HS1	-1.398
	7	THO	-1.713	THO	-1.657	THO	-2.694	THO	-2.282
$T_{max}, T_{min}, RH, R_s$	1	LGB7	1.272	LGB7	1.219	LGB7	1.177	LGB7	1.235
	2	RF7	1.230	RF7	1.206	RF7	1.168	RF7	1.227
	3	XGB7	1.162	XGB7	1.180	XGB7	1.156	XGB7	1.199
	4	TUR	0.731	TUR	0.361	TUR	0.880	TUR	0.854
	5	VA2	0.177	VA2	-0.368	VA2	0.760	VA2	0.638
	6	VA1	-1.113	VA1	-0.455	COP	-1.439	COP	-1.656
	7	COP	-2.728	COP	-2.781	VA1	-2.823	VA1	-2.643

Table 14. Comparison of the empirical models with conventional ML models (Sub-humid).

Inputs used	RANK	Faizabad		Jabalpur		Raipur		Ranchi		Ranichauri		Samastipur	
		MODEL	GPI	MODEL	GPI	MODEL	GPI	MODEL	GPI	MODEL	GPI	MODEL	GPI
$T_{max}, T_{min}, RH, U_2$	1	LGB13	1.535	LGB13	1.502	LGB13	1.523	LGB13	1.860	LGB13	1.763	LGB13	1.425
	2	RF13	1.517	RF13	1.465	RF13	1.498	RF13	1.746	RF13	1.705	RF13	1.404
	3	XGB13	1.507	XGB13	1.458	XGB13	1.487	XGB13	1.690	XGB13	1.668	XGB13	1.317
	4	PEN	-0.909	PEN	-0.982	PEN	-0.970	PEN	-1.665	ALB	-1.308	PEN	-0.827
	5	MAH	-1.687	MAH	-1.336	MAH	-1.433	ALB	-1.720	MAH	-1.590	MAH	-1.464
	6	ALB	-1.962	ALB	-2.107	ALB	-2.104	MAH	-1.910	PEN	-2.237	ALB	-1.854
T_{max}, T_{min}, R_s	1	LGB5	1.303	LGB5	1.210	LGB5	1.280	LGB5	0.960	LGB5	0.913	LGB5	1.536
	2	RF5	1.211	RF5	1.175	RF5	1.253	RF5	0.924	RF5	0.882	RF5	1.496
	3	XGB5	1.196	XGB5	1.156	XGB5	1.189	XGB5	0.918	XGB5	0.881	XGB5	1.490
	4	JH	0.465	PT	0.064	PT	0.002	PT	0.582	MAK	0.424	JH	-0.090
	5	PT	-0.483	JH	-0.131	JH	-0.141	MAK	0.159	JH	0.058	PT	-0.749
	6	MAK	-1.162	MAK	-0.684	MAK	-0.862	JH	-0.503	PT	-0.071	MAK	-1.365
	7	MGB	-2.530	MGB	-2.790	MGB	-2.720	MGB	-3.040	MGB	-3.087	MGB	-2.318
T_{max}, T_{min}, R_a	1	LGB6	1.866	LGB6	1.741	LGB6	1.716	LGB6	1.517	LGB6	1.138	LGB6	1.917
	2	XGB6	1.615	RF6	1.613	RF6	1.531	RF6	1.280	RF6	0.992	XGB6	1.559
	3	RF6	1.593	XGB6	1.539	XGB6	1.523	XGB6	1.226	XGB6	0.960	RF6	1.535
	4	HS	-0.667	HS	-0.636	HS	-0.367	HS	-0.514	HS	0.522	HS	-0.772
	5	HS1	-1.265	THO	-1.342	HS1	-1.161	THO	-0.632	HS2	0.036	HS1	-1.147
	6	HS2	-1.365	HS1	-1.386	HS2	-1.201	HS1	-1.429	HS1	-0.785	HS2	-1.246
	7	THO	-1.777	HS2	-1.530	THO	-2.040	HS2	-1.448	THO	-2.862	THO	-1.845
$T_{max}, T_{min}, RH, R_s$	1	LGB7	0.946	LGB7	1.071	RF7	1.063	LGB7	1.156	LGB7	0.979	LGB7	1.141
	2	RF7	0.938	RF7	1.063	LGB7	1.061	RF7	1.132	RF7	0.966	RF7	1.131
	3	XGB7	0.875	XGB7	1.039	XGB7	1.021	XGB7	1.103	XGB7	0.962	XGB7	1.120
	4	TUR	0.477	TUR	0.675	TUR	0.544	TUR	0.724	VA2	0.794	TUR	0.143
	5	VA2	0.275	VA2	0.436	VA2	0.387	VA2	0.441	TUR	0.776	VA2	-0.028
	6	COP	-0.457	COP	-1.354	COP	-1.139	VA1	-1.982	COP	-2.163	COP	-0.648
	7	VA1	-3.054	VA1	-2.929	VA1	-2.937	COP	-2.574	VA1	-2.312	VA1	-2.859

3.4. Comparison of Various Input Combinations in GWO Hybrid ML Models

3.4.1. Best-Performing Models in Hybrid ML

The results of the best hyperparameters in each of the models are attached in Tables S13 to S18. These hyperparameters were used to develop the hybrid ML models at all the stations of humid and sub-humid zones. The statistical indicators at each of the stations using the hybrid ML models are given in Tables S19–S28. The six accurate models in each of the ML models were employed in assessing the best-performing models. The ranking of the best of all the hybrid ML models and their combinations at humid locations based on the GPI is shown in Table 15. The results indicated that the models that used the most inputs (Index 17 and 18) were superior with higher GPI. The GWOXGB17 and GWOXGB18 performed best in all the stations, whereas the GWOLGB18 was the second best at Palampur and Thrissur. It was observed that indices 7, 8, and 9, which solar radiation data performed better in most of the stations. The superiority of RF models in these combinations was observed in all the stations except at Thrissur. The performance of the model GWOXGB18 at Thrissur was the best of the models with an RMSE of 0.073 mm/day and R^2 of 0.997.

Of the 54 hybrid models evaluated, the eighteen best-ranking hybrid ML models at sub-humid locations are shown in Table 16. The performance of the models was in the order of indices: 17, 18, and 16 at the Faizabad, Jabalpur, and Raipur stations. The accuracy of the models with indices 7, 8, and 9 is also high compared to the models that used a higher number of inputs. This could be attributed to the incorporation of solar radiation data. The model indices 15 and 13 also found a place in the best-performing models, with wind speed as a common input. The lowest RMSE (0.083 mm/day) was observed at Ranichauri, which used GWOLGB17, while the R^2 was found to be the highest (0.997) at Jabalpur for both GWOLGB18 and GWOLGB17. The overall performance of the hybrid models is in the order of GWOXGB > GWOLGB > GWORF at most stations.

Table 15. Ranking of the best-performing GWO–ML models at humid stations.

RANK	Jorhat		Mohanpur		Palampur		Thrissur	
	MODEL	GPI	MODEL	GPI	MODEL	GPI	MODEL	GPI
1	GWOXGB17	2.175	GWOXGB17	2.176	GWOXGB18	2.078	GWOXGB18	1.376
2	GWOXGB18	2.134	GWOXGB18	2.072	GWOLGB18	2.078	GWOLGB18	1.360
3	GWOLGB18	1.843	GWOLGB17	2.052	GWOXGB17	2.038	GWOXGB17	1.287
4	GWOLGB17	1.747	GWOLGB18	1.798	GWOLGB17	2.030	GWOLGB17	1.271
5	GWOXGB8	0.854	GWORF17	1.209	GWORF18	1.621	GWORF17	0.820
6	GWORF17	0.530	GWORF18	1.079	GWORF17	1.466	GWORF18	0.687
7	GWOLGB8	0.469	GWOXGB8	0.812	GWOXGB7	−0.197	GWOLGB16	0.220
8	GWORF18	0.313	GWOLGB8	0.731	GWOLGB7	−0.207	GWOXGB16	0.183
9	GWORF8	0.041	GWORF8	0.421	GWORF7	−0.252	GWOLGB8	0.101
10	GWORF9	−0.167	GWORF9	0.357	GWOLGB16	−0.457	GWOXGB8	0.059
11	GWOLGB12	−0.835	GWOLGB9	−1.312	GWOXGB16	−0.468	GWORF16	−0.103
12	GWOLGB9	−0.886	GWOXGB9	−1.368	GWORF16	−0.705	GWORF8	−0.123
13	GWOXGB9	−0.912	GWOLGB12	−1.496	GWOLGB8	−1.258	GWORF9	−0.203
14	GWORF12	−0.971	GWORF12	−1.599	GWORF8	−1.295	GWOXGB15	−0.513
15	GWOXGB12	−0.983	GWOLGB7	−1.673	GWORF9	−1.318	GWOLGB15	−0.538
16	GWOLGB7	−1.765	GWOXGB12	−1.726	GWOXGB8	−1.372	GWORF15	−0.650
17	GWOXGB7	−1.782	GWOXGB7	−1.749	GWOLGB12	−1.861	GWOLGB7	−2.610
18	GWORF7	−1.807	GWORF7	−1.786	GWOXGB12	−1.922	GWOXGB7	−2.624

3.4.2. Least Performing Models in Hybrid ML

The least-performing models of the hybrid ML at humid stations are presented in Table 17. The six least accurate models in each hybrid ML, i.e., GWORF, GWOXGB, and GWOLGB, were used to analyse all the combinations. The models with the lowest GPI values were found in the order of the model indices 1, 3, and 6 in all the hybrid ML at most stations. The models with indices 10 and 11 that used extra-terrestrial radiation as input were also placed in the least-ranking hybrid models at all the stations. There was no specific order found in the accuracy of the various models. The performance ranking of the least accurate hybrid models is given in Table 18. The model GWORF1 at Thrissur station gave the highest RMSE (0.812 mm/day) of all the models, whereas the lowest R² (0.478) was observed at Jorhat stations with the same model combination.

The least ranked models in the sub-humid stations were similar to that of the results of humid stations. Models 1, 2, 3, and 6 were the least accurate in most sub-humid locations. Of the four input combination methods, the models with the indices 10, 14, 11, and 13 found a place in the least ranked models. The performance of the different hybrid models did not show any specific trend at this level of comparison in all the stations. The error was observed highest (1.154 mm/day) at Faizabad for both GWOLGB1 and GWOXGB1. The R² was found to be the least at Samastipur station, with a value of 0.693. The RF models have got the advantage of improving their efficiency by the hyperparameter tuning by GWO than the XGB and LGB models.

Table 16. Ranking of the best-performing GWO–ML models at sub-humid stations.

RANK	Faizabad		Jabalpur		Raipur		Ranchi		Ranichauri		Samastipur	
	MODEL	GPI	MODEL	GPI	MODEL	GPI	MODEL	GPI	MODEL	GPI	MODEL	GPI
1	GWOXGB17	1.865	GWOLGB18	1.366	GWOXGB17	1.412	GWOXGB18	1.856	GWOLGB17	2.504	GWOXGB17	1.985
2	GWOXGB18	1.855	GWOXGB18	1.361	GWOXGB18	1.384	GWOXGB17	1.847	GWOXGB17	2.486	GWOLGB17	1.982
3	GWOLGB17	1.826	GWOLGB17	1.360	GWOLGB17	1.332	GWOLGB17	1.747	GWOLGB18	2.476	GWOXGB18	1.883
4	GWOLGB18	1.759	GWOXGB17	1.350	GWOLGB18	1.310	GWOLGB18	1.696	GWOXGB18	2.439	GWOLGB18	1.868
5	GWORF17	1.207	GWORF17	0.900	GWORF17	0.929	GWORF17	0.996	GWORF18	1.547	GWORF17	1.286
6	GWORF18	1.160	GWORF18	0.877	GWORF18	0.866	GWORF18	0.947	GWORF17	1.393	GWORF18	0.985
7	GWOLGB16	0.215	GWOLGB16	0.378	GWOXGB16	0.519	GWOXGB8	0.348	GWOLGB7	0.060	GWOLGB8	0.186
8	GWOXGB16	0.176	GWOXGB16	0.358	GWOLGB16	0.483	GWOLGB8	0.321	GWOXGB7	0.054	GWOXGB8	0.122
9	GWOXGB8	−0.214	GWORF16	0.007	GWORF16	0.149	GWORF8	0.166	GWORF7	−0.176	GWORF8	0.011
10	GWOLGB8	−0.255	GWOXGB8	−0.009	GWOLGB8	−0.113	GWORF9	0.063	GWOLGB8	−1.359	GWORF9	0.004
11	GWORF8	−0.359	GWOLGB8	−0.013	GWOXGB8	−0.142	GWOXGB16	−0.338	GWOXGB8	−1.365	GWOLGB16	−0.653
12	GWORF9	−0.376	GWORF8	−0.092	GWORF8	−0.259	GWOLGB16	−0.423	GWOLGB9	−1.369	GWOXGB16	−0.762
13	GWORF16	−0.447	GWORF9	−0.201	GWORF9	−0.363	GWORF16	−0.904	GWOLGB12	−1.399	GWORF16	−0.894
14	GWOXGB15	−1.269	GWOXGB15	−0.724	GWOXGB15	−0.730	GWOXGB15	−1.253	GWOXGB9	−1.422	GWOXGB7	−1.330
15	GWOLGB15	−1.325	GWOLGB15	−0.764	GWOLGB15	−0.762	GWOLGB15	−1.304	GWOXGB12	−1.455	GWOLGB7	−1.357
16	GWORF15	−1.679	GWORF15	−0.898	GWORF15	−0.903	GWORF15	−1.488	GWORF9	−1.457	GWORF7	−1.475
17	GWOXGB13	−2.011	GWOLGB13	−2.625	GWOXGB13	−2.522	GWOLGB12	−2.131	GWORF12	−1.464	GWOLGB15	−1.837
18	GWOLGB13	−2.128	GWOXGB13	−2.630	GWOLGB13	−2.588	GWOXGB12	−2.144	GWORF8	−1.496	GWOXGB9	−2.001

Table 17. Ranking of the least-performing GWO–ML models at humid stations.

RANK	Jorhat		Mohanpur		Palampur		Thrissur	
	MODEL	GPI	MODEL	GPI	MODEL	GPI	MODEL	GPI
54	GWORF1	−1.832	GWOXGB1	−2.195	GWOXGB1	−2.715	GWOXGB1	−2.220
53	GWOLGB1	−1.798	GWOLGB1	−2.163	GWOLGB1	−2.690	GWORF1	−2.217
52	GWOXGB1	−1.789	GWORF1	−2.158	GWORF1	−2.666	GWOLGB1	−2.183
51	GWOLGB3	−0.965	GWORF2	−1.330	GWOXGB3	−0.542	GWORF6	−1.687
50	GWORF3	−0.944	GWOLGB2	−1.314	GWOLGB3	−0.523	GWOLGB6	−1.648
49	GWOXGB3	−0.802	GWOXGB2	−1.142	GWORF3	−0.513	GWOXGB6	−1.584
48	GWORF6	−0.413	GWORF3	−0.257	GWORF6	−0.002	GWORF2	0.139
47	GWOXGB6	−0.361	GWOXGB3	0.095	GWOXGB6	0.044	GWOLGB2	0.172
46	GWOLGB6	−0.339	GWOLGB3	0.159	GWOLGB6	0.131	GWOXGB2	0.180
45	GWORF11	−0.271	GWORF6	0.487	GWORF4	0.922	GWORF10	0.422
44	GWOLGB11	−0.189	GWOLGB6	0.576	GWORF4	0.924	GWOLGB10	0.475
43	GWOXGB11	0.065	GWOXGB6	0.600	GWOXGB11	0.953	GWOXGB10	0.490
42	GWORF2	1.016	GWORF13	0.955	GWOLGB4	0.957	GWORF3	1.447
41	GWOLGB2	1.072	GWOLGB13	1.301	GWORF11	1.066	GWOLGB3	1.495
40	GWOXGB2	1.139	GWOXGB13	1.362	GWOLGB11	1.070	GWOXGB3	1.503
39	GWORF10	2.119	GWORF10	1.560	GWORF2	1.108	GWORF11	1.711
38	GWOLGB10	2.134	GWOLGB10	1.679	GWOXGB2	1.234	GWOXGB13	1.727
37	GWOXGB10	2.157	GWOXGB11	1.786	GWOLGB2	1.241	GWOLGB13	1.777

Table 18. Ranking of the least-performing GWO–ML models at sub-humid stations.

RANK	Faizabad		Jabalpur		Raipur		Ranchi		Ranichauri		Samastipur	
	MODEL	GPI	MODEL	GPI	MODEL	GPI	MODEL	GPI	MODEL	GPI	MODEL	GPI
54	GWOXGB1	−2.067	GWOXGB1	−2.069	GWOXGB1	−2.052	GWOXGB2	−1.696	GWOLGB1	−2.296	GWOLGB1	−2.328
53	GWOLGB1	−2.059	GWORF1	−2.025	GWOLGB1	−2.029	GWOLGB2	−1.618	GWORF1	−2.272	GWORF1	−2.322
52	GWORF1	−1.942	GWOLGB1	−2.018	GWORF1	−1.977	GWORF2	−1.599	GWOXGB1	−2.257	GWOXGB1	−2.276
51	GWORF6	−0.563	GWORF2	−1.151	GWOXGB2	−0.901	GWOXGB1	−1.542	GWORF3	−1.348	GWORF6	−0.666
50	GWOLGB2	−0.460	GWOXGB2	−1.084	GWORF2	−0.900	GWORF1	−1.535	GWOLGB3	−1.296	GWOLGB6	−0.583
49	GWOLGB6	−0.404	GWOLGB2	−1.063	GWOLGB2	−0.853	GWOLGB1	−1.535	GWOXGB3	−1.218	GWOXGB6	−0.552
48	GWOXGB2	−0.402	GWOXGB6	−0.375	GWOLGB6	−0.579	GWORF10	−0.354	GWORF2	0.031	GWOXGB2	−0.230
47	GWOXGB6	−0.373	GWORF6	−0.300	GWOXGB6	−0.548	GWORF6	−0.304	GWOXGB2	0.032	GWORF2	−0.195
46	GWORF2	−0.252	GWOLGB6	−0.273	GWORF6	−0.514	GWOXGB10	−0.148	GWOLGB2	0.046	GWOLGB2	−0.165
45	GWORF4	−0.238	GWOXGB10	0.356	GWOXGB10	0.422	GWOLGB10	−0.106	GWORF6	0.776	GWOXGB3	0.321
44	GWOXGB4	−0.143	GWORF10	0.462	GWORF10	0.429	GWOXGB6	−0.023	GWOLGB6	0.790	GWOLGB3	0.337
43	GWOLGB4	−0.139	GWOLGB10	0.503	GWOLGB10	0.534	GWOLGB6	0.035	GWOXGB6	0.799	GWORF3	0.368
42	GWOXGB14	1.105	GWORF4	1.126	GWORF4	1.036	GWORF3	1.161	GWORF13	0.956	GWORF11	1.073
41	GWOLGB14	1.180	GWOXGB4	1.265	GWOLGB4	1.083	GWOXGB3	1.365	GWOLGB13	1.136	GWOXGB11	1.127
40	GWORF14	1.239	GWOLGB4	1.286	GWOXGB4	1.108	GWOLGB3	1.404	GWOXGB13	1.143	GWOLGB11	1.240
39	GWOXGB10	1.791	GWORF14	1.757	GWOXGB14	1.904	GWORF13	1.959	GWORF11	1.640	GWORF10	1.534
38	GWORF5	1.817	GWOXGB14	1.782	GWORF14	1.915	GWOXGB13	2.237	GWOXGB11	1.645	GWOLGB10	1.651
37	GWOLGB10	1.909	GWOLGB3	1.823	GWOLGB14	1.922	GWOLGB13	2.299	GWOLGB11	1.692	GWOXGB10	1.665

3.5. Best-Performing Models across Conventional and Hybrid MLs

Table 19 depicts the best 36 models out of 108 models that compare all the conventional and hybrid ML at humid locations. The plots showing the RMSE and R^2 at different locations in the humid region are shown in Figures 4 and 5, respectively. The results indicate that the hybrid models outperformed their conventional ML counterparts in most of the combinations. The models that used the six inputs were the superior, followed by the models with indices 7, 8, 9, 16, and 12. The accuracy of the XGB and LGB models was higher than RF models at almost all stations. The use of solar radiation could be attributed to the excellent performance of models 7, 8, and 9 than the other models that have employed more inputs.

Table 19. Ranking of the best-performing models in conventional and hybrid MLs at humid stations.

RANK	Jorhat		Mohanpur		Palampur		Thrissur	
	MODEL	GPI	MODEL	GPI	MODEL	GPI	MODEL	GPI
1	GWOXGB17	2.031	GWOXGB17	2.077	GWOXGB18	1.953	GWOXGB18	1.302
2	GWOXGB18	1.995	GWOXGB18	1.982	GWOLGB18	1.953	GWOLGB18	1.288
3	GWOLGB18	1.740	GWOLGB17	1.964	GWOXGB17	1.916	GWOXGB17	1.222
4	GWOLGB17	1.656	GWOLGB18	1.732	GWOLGB17	1.909	GWOLGB17	1.207
5	XGB17	1.538	XGB17	1.635	LGB18	1.810	LGB18	1.062
6	XGB18	1.419	LGB17	1.633	LGB17	1.754	LGB17	1.051
7	LGB17	1.388	LGB18	1.439	XGB18	1.642	XGB17	1.025
8	LGB18	1.388	XGB18	1.413	XGB17	1.621	XGB18	0.987
9	GWOXGB8	0.869	GWORF17	1.193	GWORF18	1.537	GWORF17	0.799
10	GWORF17	0.589	RF17	1.176	RF18	1.528	RF17	0.793
11	RF17	0.579	GWORF18	1.075	GWORF17	1.395	GWORF18	0.679
12	GWOLGB8	0.533	RF18	1.054	RF17	1.376	RF18	0.661
13	XGB8	0.533	GWOXGB8	0.829	GWOXGB7	−0.110	GWOLGB16	0.252
14	LGB8	0.510	GWOLGB8	0.755	GWOLGB7	−0.119	GWOXGB16	0.220
15	GWORF18	0.399	LGB8	0.673	LGB7	−0.129	LGB16	0.152
16	RF18	0.392	XGB8	0.540	GWORF7	−0.159	GWOLGB8	0.150
17	GWORF8	0.159	GWORF8	0.473	RF7	−0.210	GWOXGB8	0.112
18	RF8	0.148	RF9	0.454	XGB7	−0.318	LGB8	0.063
19	RF9	0.144	RF8	0.445	GWOLGB16	−0.348	XGB16	0.015
20	GWORF9	−0.023	GWORF9	0.414	GWOXGB16	−0.358	XGB8	0.005
21	GWOLGB12	−0.607	GWOLGB9	−1.103	LGB16	−0.393	GWORF16	−0.037
22	GWOLGB9	−0.652	GWOXGB9	−1.154	GWORF16	−0.571	GWORF8	−0.050
23	GWOXGB9	−0.675	LGB9	−1.169	RF16	−0.577	RF16	−0.065
24	GWORF12	−0.726	GWOLGB12	−1.270	XGB16	−0.673	RF8	−0.069
25	GWOXGB12	−0.736	LGB12	−1.313	GWOLGB8	−1.068	RF9	−0.075
26	LGB12	−0.739	GWORF12	−1.363	GWORF8	−1.101	GWORF9	−0.123
27	LGB9	−0.762	RF12	−1.376	LGB8	−1.102	GWOXGB15	−0.407
28	RF12	−1.040	GWOLGB7	−1.433	GWORF9	−1.122	GWOLGB15	−0.430
29	XGB9	−1.208	LGB7	−1.469	GWOXGB8	−1.171	LGB15	−0.445
30	XGB12	−1.288	GWOXGB12	−1.478	RF8	−1.218	GWORF15	−0.529
31	GWOLGB7	−1.422	GWOXGB7	−1.501	RF9	−1.238	RF15	−0.561
32	GWOXGB7	−1.436	GWORF7	−1.535	XGB8	−1.394	XGB15	−0.581
33	GWORF7	−1.458	XGB9	−1.537	GWOLGB12	−1.611	GWOLGB7	−2.275
34	LGB7	−1.564	RF7	−1.617	GWOXGB12	−1.665	GWOXGB7	−2.288
35	RF7	−1.717	XGB12	−1.712	LGB12	−1.694	LGB7	−2.413
36	XGB7	−1.958	XGB7	−1.923	XGB12	−2.047	XGB7	−2.698

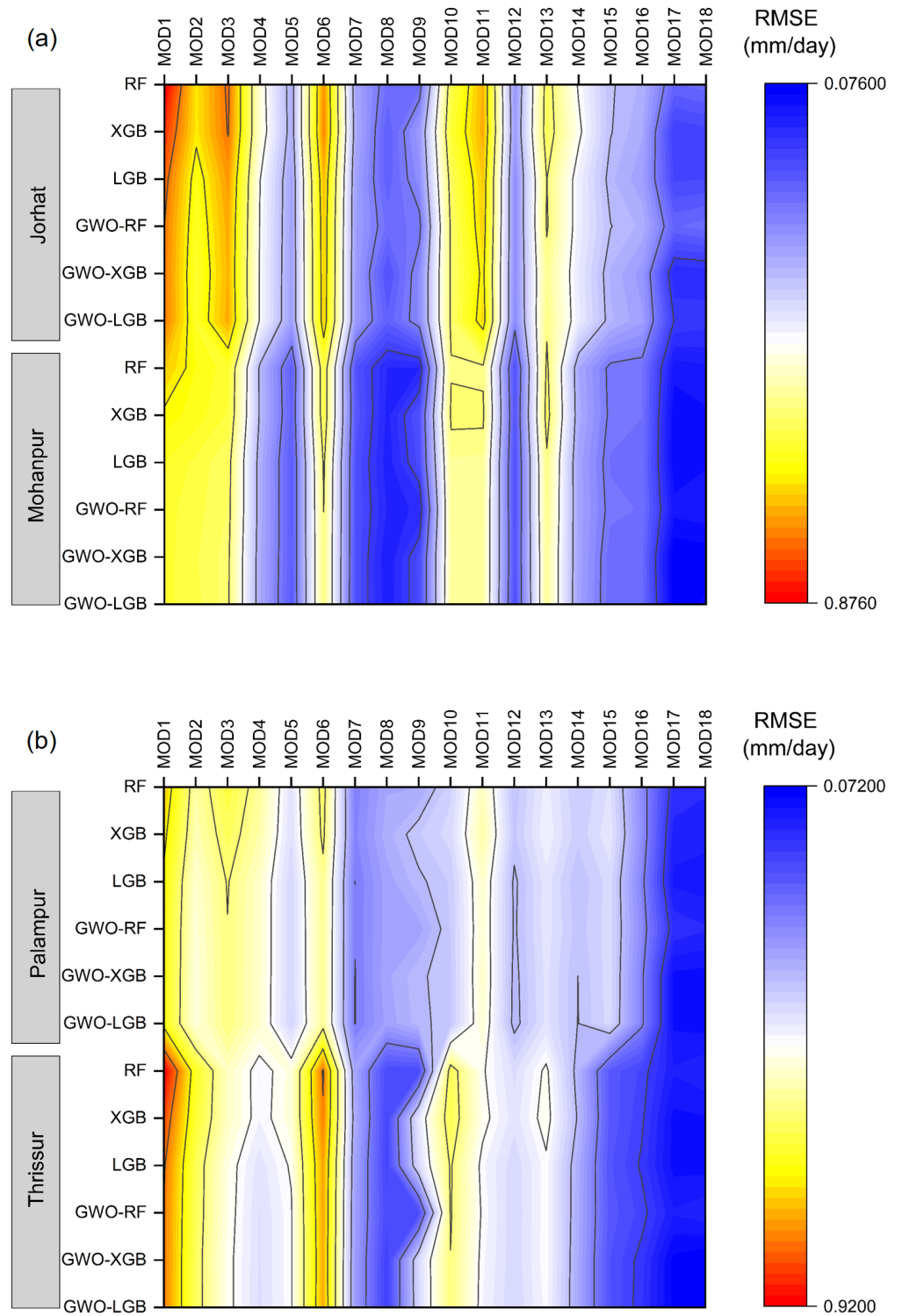


Figure 4. RMSE (mm/day) at humid locations of all ML models at (a) Jorhat, and Mohanpur; (b) Palampur, and Thrissur.

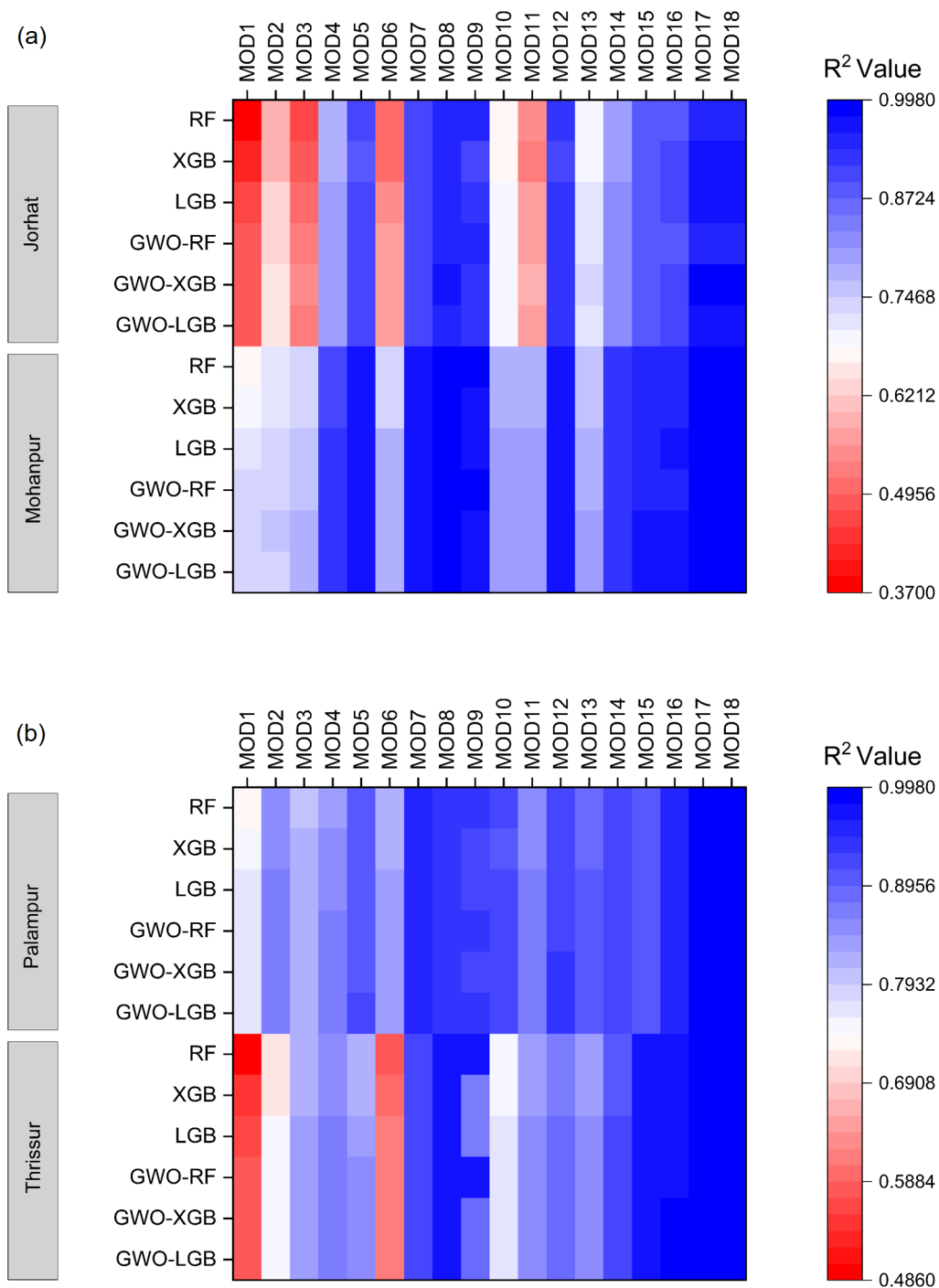
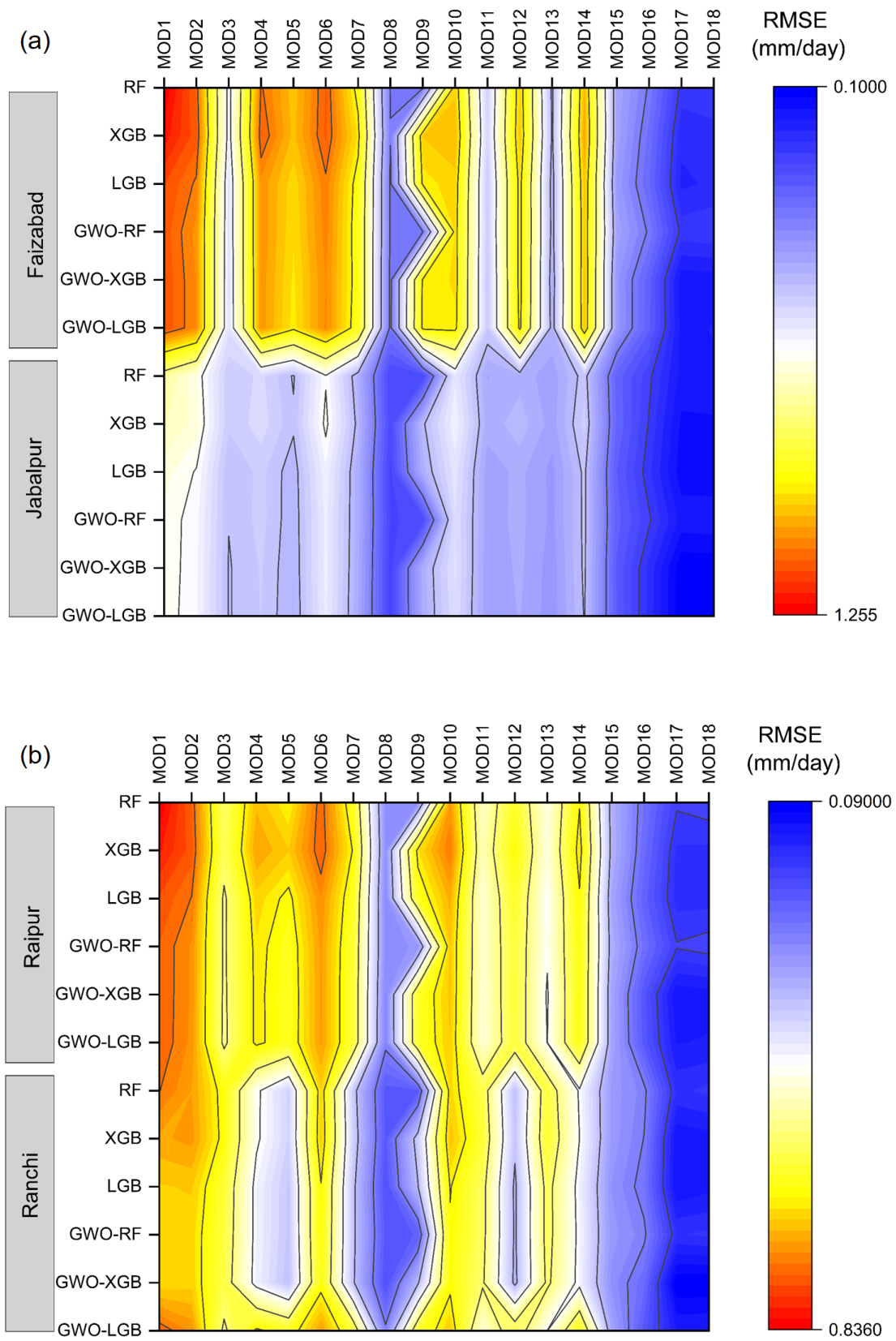


Figure 5. R² values at humid locations of all ML models at (a) Jorhat, and Mohanpur; (b) Palampur, and Thrissur.

The results of the overall best-performing models in conventional and hybrid models at the sub-humid stations are presented in Table 20. The plots showing the RMSE and R² at different locations in the humid region are shown in Figures 6 and 7, respectively. The observed results at the sub-humid locations were in good resonance with that of the humid locations. The models with indices 17, 18, and 16 were also predicting with greater accuracy at these locations. The solar radiation data used in models 7, 8, and 9 were also ranked best in comparison. The application of GWO has improved the accuracy of the ML models in all the combinations at all stations. The higher GPI values were observed in LGB and XGB when compared with the RF models using a similar set of inputs.

Table 20. Ranking of the best-performing models in conventional and hybrid MLs at sub-humid stations.

RANK	Faizabad		Jabalpur		Raipur		Ranchi		Ranichauri		Samastipur	
	MODEL	GPI	MODEL	GPI	MODEL	GPI	MODEL	GPI	MODEL	GPI	MODEL	GPI
1	GWOXGB17	1.810	GWOLGB18	1.315	GWOXGB17	1.368	GWOXGB18	1.739	GWOLGB17	2.383	GWOXGB17	1.944
2	GWOXGB18	1.801	GWOXGB18	1.311	GWOXGB18	1.343	GWOXGB17	1.731	GWOXGB17	2.366	GWOLGB17	1.941
3	GWOLGB17	1.774	GWOLGB17	1.310	GWOLGB17	1.295	GWOLGB17	1.642	GWOLGB18	2.357	GWOXGB18	1.847
4	GWOLGB18	1.711	GWOXGB17	1.301	GWOLGB18	1.273	GWOLGB18	1.595	GWOXGB18	2.323	GWOLGB18	1.834
5	LGB17	1.556	LGB18	1.146	LGB18	1.120	LGB17	1.434	LGB17	2.136	LGB17	1.726
6	LGB18	1.491	LGB17	1.104	LGB17	1.105	XGB17	1.394	LGB18	2.069	LGB18	1.644
7	XGB17	1.443	XGB18	1.025	XGB18	1.056	LGB18	1.369	XGB17	1.980	XGB17	1.588
8	XGB18	1.378	XGB17	1.023	XGB17	1.052	XGB18	1.352	XGB18	1.818	XGB18	1.421
9	RF17	1.203	GWORF17	0.887	GWORF17	0.921	RF17	0.985	GWORF18	1.505	GWORF17	1.284
10	GWORF17	1.199	RF17	0.887	RF17	0.907	GWORF17	0.964	RF18	1.499	RF17	1.245
11	GWORF18	1.155	GWORF18	0.866	GWORF18	0.863	GWORF18	0.921	GWORF17	1.364	GWORF18	1.002
12	RF18	1.155	RF18	0.860	RF18	0.849	RF18	0.910	RF17	1.347	RF18	0.909
13	GWOLGB16	0.278	GWOLGB16	0.406	GWOXGB16	0.540	GWOXGB8	0.382	GWOLGB7	0.144	GWOLGB8	0.247
14	GWOXGB16	0.241	GWOXGB16	0.388	GWOLGB16	0.507	GWOLGB8	0.358	GWOXGB7	0.139	LGB8	0.194
15	LGB16	0.073	LGB16	0.270	LGB16	0.381	LGB8	0.357	LGB7	0.114	GWOXGB8	0.187
16	XGB16	-0.103	XGB16	0.125	XGB16	0.241	RF8	0.226	GWORF7	-0.071	GWORF8	0.083
17	GWOXGB8	-0.119	GWORF16	0.066	GWORF16	0.199	GWORF8	0.219	RF7	-0.094	GWORF9	0.077
18	GWOLGB8	-0.157	GWOXGB8	0.053	RF16	0.169	RF9	0.210	XGB7	-0.156	RF9	0.055
19	LGB8	-0.196	GWOLGB8	0.050	GWOLGB8	-0.042	XGB8	0.189	GWOLGB8	-1.152	RF8	0.048
20	RF9	-0.225	RF16	0.045	GWOXGB8	-0.069	GWORF9	0.127	GWOXGB8	-1.158	XGB8	-0.038
21	GWORF8	-0.253	LGB8	0.014	LGB8	-0.128	GWOXGB16	-0.234	GWOLGB9	-1.161	GWOLGB16	-0.541
22	RF8	-0.262	GWORF8	-0.022	GWORF8	-0.175	GWOLGB16	-0.310	LGB9	-1.178	LGB16	-0.627
23	GWORF9	-0.269	RF8	-0.047	RF9	-0.185	LGB16	-0.432	LGB8	-1.183	GWOXGB16	-0.642
24	GWORF16	-0.335	RF9	-0.047	RF8	-0.193	XGB16	-0.624	GWOLGB12	-1.189	GWORF16	-0.767
25	RF16	-0.348	GWORF9	-0.121	XGB8	-0.243	GWORF16	-0.741	GWOXGB9	-1.210	RF16	-0.779
26	XGB8	-0.358	XGB8	-0.135	GWORF9	-0.272	RF16	-0.760	GWOXGB12	-1.240	XGB16	-0.913
27	GWOXGB15	-1.096	GWOXGB15	-0.602	GWOXGB15	-0.612	GWOXGB15	-1.053	GWORF9	-1.242	GWOXGB7	-1.176
28	GWOLGB15	-1.148	GWOLGB15	-0.638	LGB15	-0.631	GWOLGB15	-1.098	GWORF12	-1.248	GWOLGB7	-1.201
29	LGB15	-1.196	LGB15	-0.644	GWOLGB15	-0.642	LGB15	-1.118	LGB12	-1.252	LGB7	-1.219
30	XGB15	-1.445	GWORF15	-0.760	GWORF15	-0.771	GWORF15	-1.263	GWORF8	-1.277	GWORF7	-1.312
31	GWORF15	-1.476	RF15	-0.798	RF15	-0.785	RF15	-1.323	RF9	-1.366	RF7	-1.355
32	RF15	-1.501	XGB15	-0.871	XGB15	-0.860	XGB15	-1.326	RF8	-1.393	XGB7	-1.495
33	GWOXGB13	-1.783	GWOLGB13	-2.335	GWOXGB13	-2.261	GWOLGB12	-1.831	RF12	-1.420	GWOLGB15	-1.653
34	GWOLGB13	-1.891	GWOXGB13	-2.340	GWOLGB13	-2.322	GWOXGB12	-1.843	XGB9	-1.461	LGB15	-1.695
35	LGB13	-1.923	LGB13	-2.411	LGB13	-2.368	LGB12	-1.888	XGB8	-1.475	GWOXGB9	-1.805
36	XGB13	-2.183	XGB13	-2.684	XGB13	-2.632	XGB12	-2.261	XGB12	-1.617	XGB12	-2.054



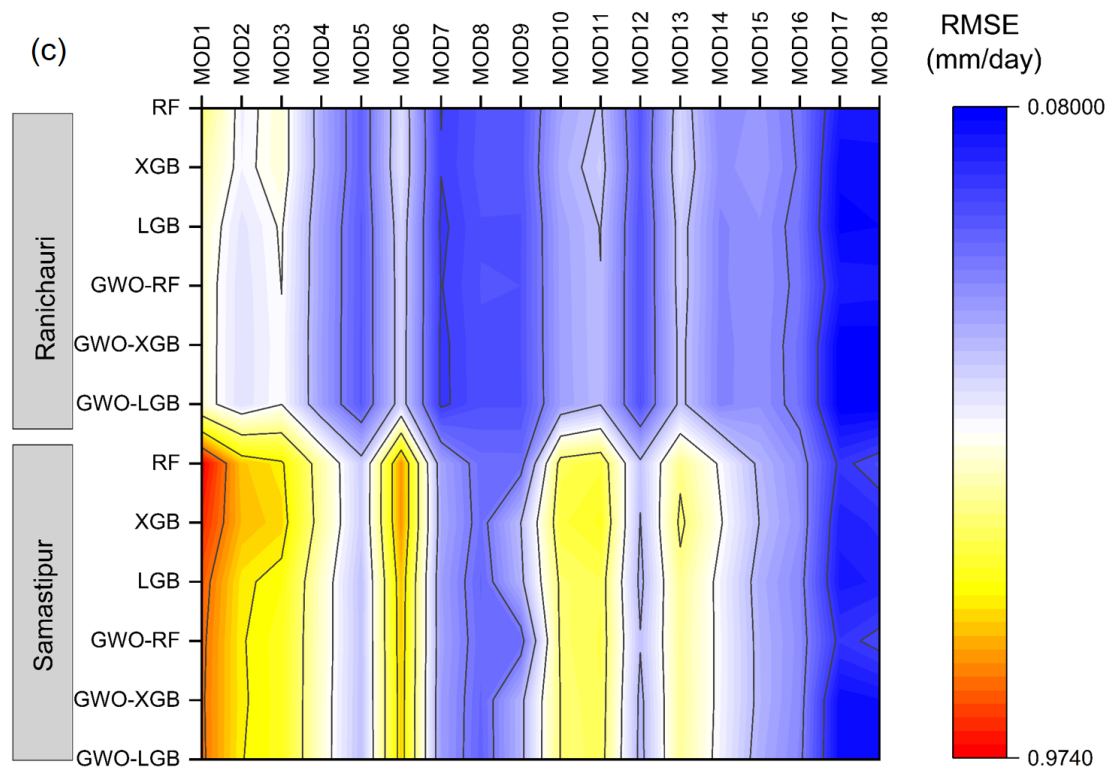


Figure 6. RMSE (mm/day) at sub-humid locations of all ML models at (a) Faizabad, and Jabalpur; (b) Raipur, and Ranchi; (c) Ranichauri, and Samastipur.

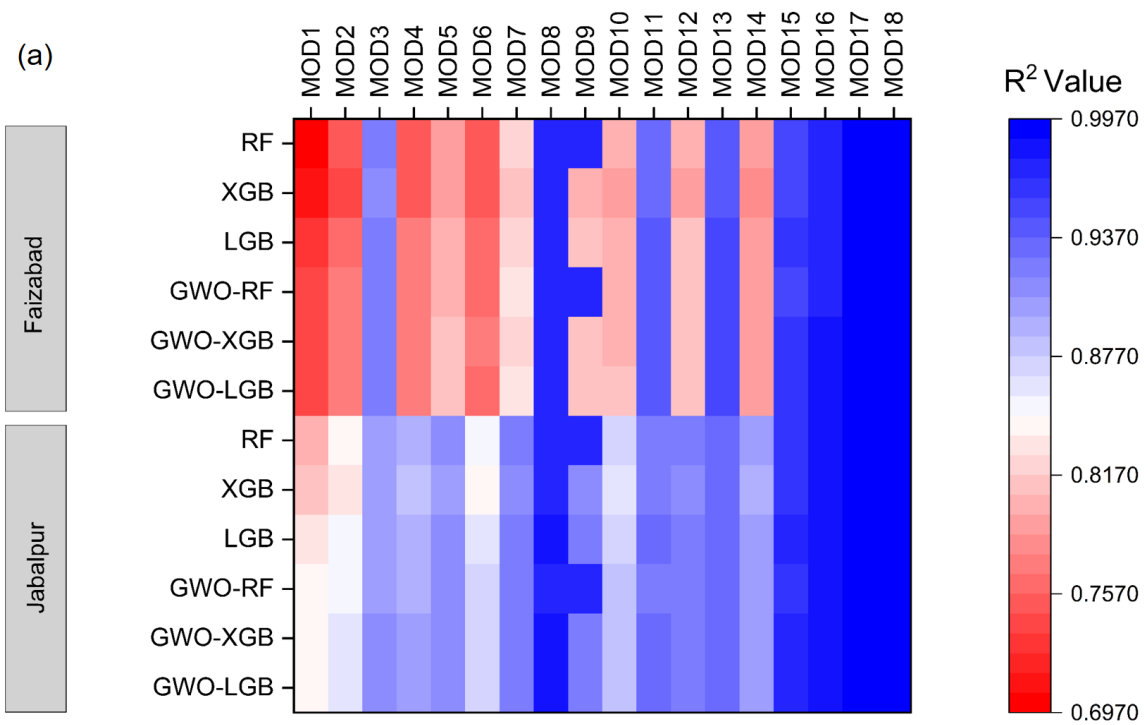


Figure 7. Cont.

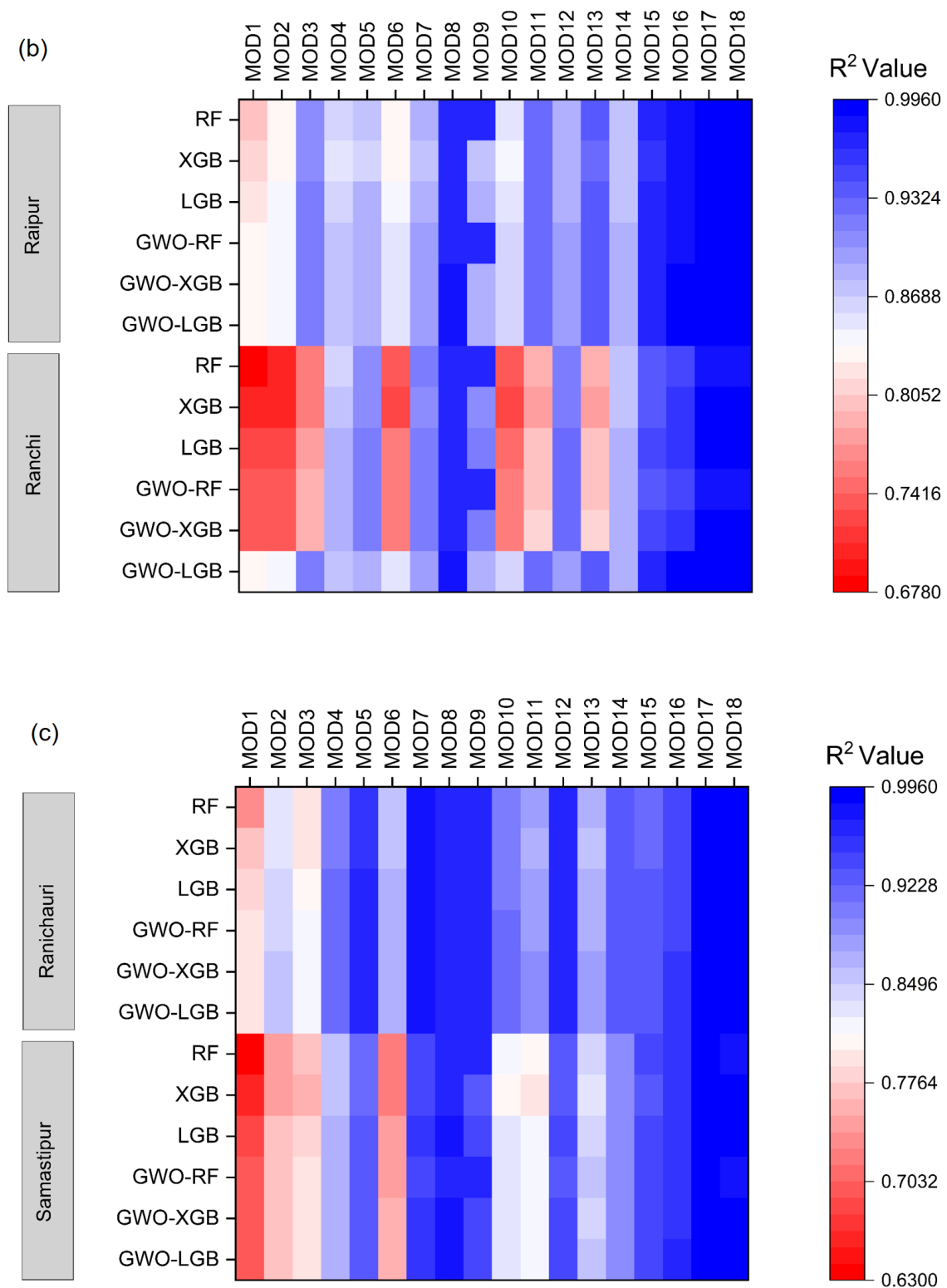


Figure 7. R^2 values at sub-humid locations of all ML models at (a) Faizabad, and Jabalpur; (b) Raipur, and Ranchi; (c) Ranichauri, and Samastipur.

3.6. Least-Performing Models across Conventional and Hybrid MLs

Based on the least GPI values, the six least-performing models from each conventional and hybrid ML model were combined to assess the ranking of all the models. Table 21 illustrates the worst ranking models at the humid stations. It was observed from the results that the models with indices 1, 2, 3, and 6 were found to be the least-ranked models. The

conventional ML models were less accurate than their hybrid models. In most instances, the XGB and LGB models were slightly more accurate than the RF models. A similar observation was noted at sub-humid locations, tabulated in Table 22. The combination of inputs that consisted of two and three inputs was the least ranked at almost all the stations. The advantage of using hybrid models could be seen with the higher GPI values of those models than the conventional ML models. The results at sub-humid locations also indicate the inferior accuracy of RF when compared to the boosting models, i.e., LGB and XGB. The addition of extra-terrestrial radiation did not increase the accuracy of the models to a greater extent, which could be observed from the model indices 10 and 11 securing least ranking than other 4-input combination models.

Table 21. Ranking of the least performing models in conventional and hybrid ML at humid stations.

RANK	Jorhat		Mohanpur		Palampur		Thrissur	
	MODEL	GPI	MODEL	GPI	MODEL	GPI	MODEL	GPI
108	RF1	−2.443	RF1	−2.685	RF1	−2.858	RF1	−2.488
107	XGB1	−1.829	XGB1	−1.645	XGB1	−2.313	XGB1	−1.934
106	LGB1	−1.374	RF2	−1.357	LGB1	−1.909	LGB1	−1.620
105	GWORF1	−1.158	XGB2	−1.176	GWOXGB1	−1.811	GWOXGB1	−1.543
104	RF3	−1.150	LGB1	−1.066	GWOLGB1	−1.793	GWORF1	−1.541
103	GWOLGB1	−1.134	GWOXGB1	−0.891	GWORF1	−1.774	RF6	−1.530
102	GWOXGB1	−1.128	GWOLGB1	−0.875	RF3	−0.956	GWOLGB1	−1.515
101	XGB3	−1.001	GWORF1	−0.871	XGB3	−0.578	XGB6	−1.380
100	XGB6	−0.703	RF3	−0.703	RF6	−0.439	LGB6	−1.144
99	LGB3	−0.655	LGB2	−0.517	XGB6	−0.266	GWORF6	−1.143
98	RF6	−0.644	XGB3	−0.455	LGB3	−0.242	GWOLGB6	−1.114
97	GWOLGB3	−0.504	GWORF2	−0.413	GWOXGB3	−0.202	GWOXGB6	−1.066
96	GWORF3	−0.488	GWOLGB2	−0.405	GWOLGB3	−0.188	RF2	−0.120
95	GWOXGB3	−0.379	GWOXGB2	−0.310	GWORF3	−0.180	XGB2	−0.006
94	XGB11	−0.264	RF6	−0.292	LGB6	0.198	XGB10	0.210
93	RF11	−0.259	XGB6	−0.212	GWORF6	0.201	LGB2	0.211
92	LGB6	−0.200	XGB13	0.163	GWOXGB6	0.235	GWORF2	0.221
91	GWORF6	−0.078	GWORF3	0.180	RF4	0.281	RF10	0.239
90	GWOXGB6	−0.040	LGB3	0.182	GWOLGB6	0.299	GWOLGB2	0.246
89	LGB11	−0.025	RF13	0.367	RF2	0.386	GWOXGB2	0.252
88	GWOLGB6	−0.024	GWOXGB3	0.374	XGB4	0.481	GWORF10	0.431
87	GWORF11	0.028	GWOLGB3	0.409	XGB11	0.511	LGB10	0.442
86	GWOLGB11	0.090	LGB6	0.446	XGB2	0.580	GWOLGB10	0.470
85	GWOXGB11	0.284	XGB10	0.513	RF11	0.744	GWOXGB10	0.481
84	RF2	0.450	GWORF6	0.593	LGB4	0.873	RF3	0.971
83	XGB2	0.484	GWOLGB6	0.640	GWORF4	0.882	XGB3	0.989
82	LGB2	0.888	GWOXGB6	0.653	GWOXGB4	0.883	LGB3	1.189
81	GWORF2	1.004	RF10	0.756	GWOXGB11	0.906	GWORF3	1.192
80	GWOLGB2	1.045	LGB13	0.804	GWOLGB4	0.908	XGB13	1.226
79	GWOXGB2	1.097	GWORF13	0.848	LGB11	0.952	GWOLGB3	1.228
78	XGB10	1.359	GWOLGB13	1.038	LGB2	0.957	GWOXGB3	1.234
77	RF10	1.540	GWOXGB13	1.071	GWORF11	0.990	RF5	1.269
76	LGB10	1.695	LGB10	1.092	GWOLGB11	0.993	GWORF11	1.387
75	GWORF10	1.826	GWORF10	1.183	GWORF2	1.019	GWOXGB13	1.398
74	GWOLGB10	1.837	GWOLGB10	1.250	GWOXGB2	1.113	LGB5	1.423
73	GWOXGB10	1.854	GWOXGB11	1.312	GWOLGB2	1.118	GWOLGB13	1.435

Table 22. Ranking of the least-performing models in conventional and hybrid MLs at sub-humid stations.

RANK	Faizabad		Jabalpur		Raipur		Ranchi		Ranichauri		Samastipur	
	MODEL	GPI	MODEL	GPI	MODEL	GPI	MODEL	GPI	MODEL	GPI	MODEL	GPI
108	RF1	-2.488	RF1	-2.511	RF1	-2.473	RF1	-2.276	RF1	-2.703	RF1	-2.620
107	XGB1	-1.954	XGB1	-1.969	XGB1	-1.909	XGB2	-1.606	XGB1	-1.931	XGB1	-2.127
106	LGB1	-1.173	LGB1	-1.330	LGB1	-1.246	RF2	-1.498	LGB1	-1.471	LGB1	-1.656
105	GWOXGB1	-1.140	XGB2	-1.304	GWOXGB1	-1.036	XGB1	-1.449	GWOLGB1	-1.322	GWOLGB1	-1.492
104	GWOLGB1	-1.135	RF2	-1.126	GWOLGB1	-1.020	LGB2	-0.861	GWORF1	-1.305	GWORF1	-1.487
103	GWORF1	-1.058	GWOXGB1	-1.119	XGB2	-1.013	LGB1	-0.823	GWOXGB1	-1.295	GWOXGB1	-1.454
102	XGB2	-0.819	GWORF1	-1.090	GWORF1	-0.986	XGB10	-0.793	RF3	-1.233	RF6	-0.818
101	RF2	-0.679	GWOLGB1	-1.086	RF2	-0.889	XGB6	-0.735	XGB3	-1.215	XGB6	-0.789
100	RF6	-0.648	XGB6	-0.719	XGB6	-0.806	GWOXGB2	-0.690	LGB3	-0.772	XGB2	-0.488
99	XGB4	-0.618	LGB2	-0.695	RF6	-0.787	GWOLGB2	-0.643	GWORF3	-0.698	RF2	-0.379
98	XGB6	-0.599	GWORF2	-0.520	LGB2	-0.574	GWORF2	-0.631	GWOLGB3	-0.665	LGB6	-0.339
97	RF4	-0.394	RF6	-0.504	XGB10	-0.372	GWOXGB1	-0.597	GWOXGB3	-0.614	GWORF6	-0.293
96	LGB2	-0.253	GWOXGB2	-0.477	GWOXGB2	-0.297	GWOLGB1	-0.593	XGB2	-0.313	GWOLGB6	-0.234
95	LGB6	-0.167	GWOLGB2	-0.463	GWORF2	-0.296	GWORF1	-0.593	RF2	-0.258	GWOXGB6	-0.212
94	GWORF6	-0.139	LGB6	-0.127	GWOLGB2	-0.266	RF6	-0.591	LGB2	0.098	XGB3	-0.131
93	GWOLGB2	-0.075	XGB10	-0.100	LGB6	-0.212	RF10	-0.427	GWOXGB2	0.203	LGB2	-0.016
92	GWOXGB2	-0.036	GWOXGB6	-0.009	GWOLGB6	-0.088	LGB10	0.005	GWORF2	0.203	GWOXGB2	0.015
91	GWOLGB6	-0.034	GWORF6	0.040	GWOXGB6	-0.068	LGB6	0.066	GWOLGB2	0.213	RF3	0.035
90	GWOXGB6	-0.014	GWOLGB6	0.057	GWORF6	-0.044	GWORF10	0.121	XGB6	0.304	GWORF2	0.040
89	GWORF2	0.063	RF10	0.236	RF10	0.040	GWORF6	0.151	RF6	0.366	GWOLGB2	0.062
88	GWORF4	0.074	LGB10	0.354	XGB4	0.152	GWOXGB10	0.246	XGB13	0.445	LGB3	0.326
87	LGB4	0.106	GWOXGB10	0.468	LGB10	0.313	XGB3	0.267	RF13	0.592	GWOXGB3	0.412
86	GWOXGB4	0.137	GWORF10	0.536	RF4	0.405	GWOLGB10	0.271	LGB6	0.645	GWOLGB3	0.423
85	GWOLGB4	0.139	GWOLGB10	0.563	GWOXGB10	0.556	RF3	0.313	GWORF6	0.696	GWORF3	0.446
84	XGB14	0.520	XGB4	0.585	GWORF10	0.559	GWOXGB6	0.321	GWOLGB6	0.706	XGB11	0.586
83	RF14	0.783	RF4	0.652	GWOLGB10	0.626	GWOLGB6	0.356	GWOXGB6	0.711	RF11	0.844
82	XGB10	0.893	GWORF4	0.964	LGB4	0.767	XGB13	0.840	GWORF13	0.810	XGB10	0.903
81	LGB14	0.967	LGB4	0.986	XGB5	0.857	LGB3	0.915	LGB13	0.825	GWORF11	0.954
80	GWOXGB14	0.967	XGB3	1.006	GWORF4	0.942	GWORF3	1.036	XGB11	0.902	GWOXGB11	0.993
79	GWOLGB14	1.017	RF3	1.014	GWOLGB4	0.972	RF13	1.075	GWOLGB13	0.927	LGB11	1.016
78	RF5	1.039	GWOXGB4	1.055	GWOXGB4	0.986	GWOXGB3	1.159	GWOXGB13	0.932	GWOLGB11	1.074
77	GWORF14	1.054	GWOLGB4	1.068	RF5	1.293	GWOLGB3	1.183	RF11	1.159	RF10	1.098
76	LGB10	1.309	LGB14	1.377	LGB14	1.387	GWORF13	1.519	LGB11	1.232	LGB10	1.271
75	GWOXGB10	1.420	GWORF14	1.378	GWOXGB14	1.504	LGB13	1.552	GWORF11	1.263	GWORF10	1.287
74	GWORF5	1.439	GWOXGB14	1.394	GWORF14	1.511	GWOXGB13	1.687	GWOXGB11	1.266	GWOLGB10	1.370
73	GWOLGB10	1.497	GWOLGB3	1.417	GWOLGB14	1.514	GWOLGB13	1.724	GWOLGB11	1.297	GWOXGB10	1.380

4. Discussion

Reference evapotranspiration estimation is essential in various applications ranging from agricultural water management, hydrological balancing across basins and water allocation, etc. The study used various empirical, ML and hybrid ML models that were tested across the humid and sub-humid stations across the Indian subcontinent. Among empirical equations, the Turc model was found to be the most reliable method in empirical models used. Similar results were reported in [62,63], wherein the radiation-based Turc model performed better. Many studies have proven that the empirical equations underperformed the ML models, which was also observed in this study. [64] assessed different artificial intelligence models with empirical models like Turc, Ritchie, Thornthwaite, and Valiantzas methods. Their results indicated the supremacy of the ML models in predicting ET_0 . The comparison between the conventional ML models based on the performance indicators showed that the XGB and LGB models showed similar accuracies. [30] have also indicated that both of these models exhibited the same model efficacy. The boosting methods were to be a potential tool for humid regions according to [65]. RF models were found to be less accurate than the other boosting models, as reported in [24,29].

The model accuracy increased as increasing the inputs, which was exhibited in most of the studies. The models that used solar radiation have performed reasonably well in both the regions, i.e., humid and sub-humid. [29] also found that the addition of solar radiation improved the accuracy. The models in the sub-humid regions that used wind speed data were found to be of better accuracy. These results were similar that were found in Bangladesh [64]. The best and least performing models' results have been found to vary slightly across the stations. However, the four input combination models, indices 7 and 8, were found to be consistently performing well in both regions. Applying these data-driven models with lower inputs could be promising for developing nations.

The hybrid ML models further enhanced the predictability of the models, which could be possible by proper hyperparameter tuning. This is evident from the observation of the improvement in the GWORF model performance over the conventional RF. RF models showed a greater improvement due to the optimization than the XGB and LGB models. A similar study by [61] reported an improvement in all the combinations of inputs when employing PSO. The hyperparameter values varied considerably in all the combinations and stations. There is no fixed set of hyperparameters for all the ML models and their input combinations that could be suggested for optimal results, as suggested in [36]. Nevertheless, these models have proven to be of good accuracy, and there is a scope for further improvement if different optimizers could be tested across the regions of the World.

5. Conclusions

This study evaluated the ET_0 modelling capabilities of tree-based ML like RF, XGB, and LGB in addition to the GWO-optimized tree-based ML for ten locations in humid and sub-humid regions across India. The daily data from 2001 to 2020 of agro-meteorological parameters like maximum temperature, minimum temperature, wind speed, relative humidity, number of sunshine hours, solar radiation and extra-terrestrial radiation were employed for modelling purposes. The FAO-56 Penman-Monteith was used as the target value. Different input combinations were tested at all the stations using a cross-validation strategy. The comparison of the empirical equations was also made for the ML that used the same input combinations. The ranking of the models based on GPI value for comparison at each level was considered. The conclusions that could be drawn from the study are below.

1. The LGB and XGB models outperformed the RF models, while all the ML models were found to be more accurate than empirical models.
2. Among the empirical methods investigated in the study, the Turc model was determined to have the greatest performance with higher GPI values.
3. Solar radiation was adjudged to be an important parameter that could improve the prediction capability.

4. The GWO hybrid ML models had the highest prediction efficiencies at all the locations, with RF models improving considerably well.
5. The study consolidated the fact that the use of optimizers would substantially reduce the modelling error.
6. Further studies could be done using cross-station data and other optimizers to improve the accuracy.

Supplementary Materials: The following supplementary information can be downloaded at: <https://www.mdpi.com/article/10.3390/w15050856/s1>, Figure S1. Statistical indicators of inputs and output used in the study; Figure S2. Time series graphs of ET_0 (mm/day) at humid (Jorhat, Thrissur) and sub-humid (Raipur, Samastipur) stations; Table S1. Performance indicators of empirical models at humid stations; Table S2. Performance indicators of empirical models at sub-humid stations; Table S3. Performance indicators of conventional ML models at Jorhat; Table S4. Performance indicators of conventional ML models at Mohanpur; Table S5. Performance indicators of conventional ML models at Palampur; Table S6. Performance indicators of conventional ML models at Thrissur; Table S7. Performance indicators of conventional ML models at Faizabad; Table S8. Performance indicators of conventional ML models at Jabalpur; Table S9. Performance indicators of conventional ML models at Raipur; Table S10. Performance indicators of conventional ML models at Ranchi; Table S11. Performance indicators of conventional ML models at Ranichauri; Table S12. Performance indicators of conventional ML models at Samastipur; Table S13. Best hyper parameters in RF models at humid stations; Table S14. Best hyper parameters in XGB models at humid stations; Table S15. Best hyper parameters in LGB models at humid stations; Table S16. Best hyper parameters in RF models at sub-humid stations; Table S17. Best hyper parameters in XGB models at sub-humid stations; Table S18. Best hyper parameters in LGB models at sub-humid stations; Table S19. Performance indicators of hybrid ML models at Jorhat; Table S20. Performance indicators of hybrid ML models at Mohanpur; Table S21. Performance indicators of hybrid ML models at Palampur; Table S22. Performance indicators of hybrid ML models at Thrissur; Table S23. Performance indicators of hybrid ML models at Faizabad; Table S24. Performance indicators of hybrid ML models at Jabalpur; Table S25. Performance indicators of hybrid ML models at Raipur; Table S26. Performance indicators of hybrid ML models at Ranchi; Table S27. Performance indicators of hybrid ML models at Ranichauri; Table S28. Performance indicators of hybrid ML models at Samastipur.

Author Contributions: Conceptualization, P.H. and K.V.R.R.; methodology, P.H., K.V.R.R. and A.S. (A. Subeesh); software, P.H., A.S. (A. Subeesh) and A.S. (Ankur Srivatsava); formal analysis, P.H. and K.V.R.R.; investigation, P.H. and A.S. (A. Subeesh); writing—original draft preparation, P.H. and K.V.R.R.; writing—review and editing, K.V.R.R., A.S. (A. Subeesh) and A.S. (Ankur Srivatsava); visualization, A.S. (A. Subeesh) and A.S. (Ankur Srivatsava); supervision, K.V.R.R. All authors have read and agreed to the published version of the manuscript.

Funding: This research received no external funding.

Data Availability Statement: The datasets generated and/or analysed during the current study are available from the corresponding author upon reasonable request.

Acknowledgments: The scholarship to the first author through the ICAR JRF/SRF scholarship from Indian Council of Agricultural Research is highly acknowledged. The authors also thank the AICRP on Agro-meteorology, CRIDA, India for providing the data required.

Conflicts of Interest: The authors declare no conflict of interest.

References

1. United Nations Department of Economic and Social Affairs, Population Division. *World Population Prospects 2022: Summary of Results*; UN DESA/POP/2022/TR/NO. 3; United Nations: New York, NY, USA, 2022.
2. Lybbert, T.J.; Sumner, D.A. Agricultural Technologies for Climate Change in Developing Countries: Policy Options for Innovation and Technology Diffusion. *Food Policy* **2012**, *37*, 114–123. [[CrossRef](#)]
3. Srilakshmi, M.; Jhaharia, D.; Gupta, S.; Yurembam, G.S.; Patle, G.T. Analysis of Spatio-Temporal Variations and Change Point Detection in Pan Coefficients in the Northeastern Region of India. *Theor. Appl. Climatol.* **2022**, *147*, 1545–1559. [[CrossRef](#)]
4. George, B.A.; Reddy, B.; Raghuwanshi, N.; Wallender, W. Decision Support System for Estimating Reference Evapotranspiration. *J. Irrig. Drain. Eng.* **2002**, *128*, 1–10. [[CrossRef](#)]

5. Srivastava, A.; Sahoo, B.; Raghuvanshi, N. Evaluation of Variable Infiltration Capacity Model and MODIS-Terra Satellite-Derived Grid-Scale Evapotranspiration Estimates in a River Basin with Tropical Monsoon-Type Climatology. *J. Irrig. Drain Eng.* **2017**, *143*, 04017028. [[CrossRef](#)]
6. Albrecht, F. Die Methoden zur Bestimmung der Verdunstung der natürlichen Erdoberfläche. *Arch. Meteorol. Geophys. Bioklimatol. Ser. B* **1950**, *2*, 1–38. [[CrossRef](#)]
7. Mahringer, W. Verdunstungsstudien am Neusiedler See. *Arch. Meteorol. Geophys. Bioklimatol. Ser. B* **1970**, *18*, 1–20. [[CrossRef](#)]
8. Penman, H.L. Natural Evaporation from Open Water, Bare Soil and Grass. *Proc. R. Soc. Lond. Ser. Math. Phys. Sci.* **1948**, *193*, 120–145.
9. Abtew, W. Evapotranspiration Measurements and Modeling for Three Wetland Systems in South Florida. *JAWRA J. Am. Water Resour. Assoc.* **1996**, *32*, 465–473. [[CrossRef](#)]
10. Hansen, S. Estimation of Potential and Actual Evapotranspiration: Paper Presented at the Nordic Hydrological Conference (Nyborg, Denmark, August—1984). *Hydrol. Res.* **1984**, *15*, 205–212. [[CrossRef](#)]
11. Rosenberg, N.J.; Blad, B.L.; Verma, S.B. *Microclimate: The Biological Environment*; John Wiley & Sons: Hoboken, NJ, USA, 1983; ISBN 0-471-06066-6.
12. McGuinness, J.L.; Bordne, E.F. *A Comparison of Lysimeter-Derived Potential Evapotranspiration with Computed Values*; US Department of Agriculture: Washington, DC, USA, 1972.
13. Priestley, C.H.B.; Taylor, R.J. On the Assessment of Surface Heat Flux and Evaporation Using Large-Scale Parameters. *Mon. Weather Rev.* **1972**, *100*, 81–92. [[CrossRef](#)]
14. Turc, L. Estimation of Irrigation Water Requirements, Potential Evapotranspiration: A Simple Climatic Formula Evolved up to Date. *Ann. Agron.* **1961**, *12*, 13–49.
15. Hargreaves, G.H. Moisture Availability and Crop Production. *Trans. ASAE* **1975**, *18*, 980–984. [[CrossRef](#)]
16. Hargreaves, G.H.; Samani, Z.A. Reference Crop Evapotranspiration from Temperature. *Appl. Eng. Agric.* **1985**, *1*, 96–99. [[CrossRef](#)]
17. Droogers, P.; Allen, R.G. Estimating Reference Evapotranspiration under Inaccurate Data Conditions. *Irrig. Drain. Syst.* **2002**, *16*, 33–45. [[CrossRef](#)]
18. Alexandris, S.; Kerkides, P.; Liakatas, A. Daily Reference Evapotranspiration Estimates by the “Copais” Approach. *Agric. Water Manag.* **2006**, *82*, 371–386. [[CrossRef](#)]
19. Valiantzas, J.D. Simple ET₀ Forms of Penman’s Equation without Wind and/or Humidity Data. II: Comparisons with Reduced Set-FAO and Other Methodologies. *J. Irrig. Drain. Eng.* **2013**, *139*, 9–19. [[CrossRef](#)]
20. Jing, W.; Yaseen, Z.M.; Shahid, S.; Saggi, M.K.; Tao, H.; Kisi, O.; Salih, S.Q.; Al-Ansari, N.; Chau, K.-W. Implementation of Evolutionary Computing Models for Reference Evapotranspiration Modeling: Short Review, Assessment and Possible Future Research Directions. *Eng. Appl. Comput. Fluid Mech.* **2019**, *13*, 811–823. [[CrossRef](#)]
21. Ayodele, T.O. Machine Learning Overview. *New Adv. Mach. Learn.* **2010**, *2*, 9–18.
22. Shiri, J.; Zounemat-Kermani, M.; Kisi, O.; Mohsenzadeh Karimi, S. Comprehensive Assessment of 12 Soft Computing Approaches for Modelling Reference Evapotranspiration in Humid Locations. *Meteorol. Appl.* **2020**, *27*, e1841. [[CrossRef](#)]
23. Bellido-Jiménez, J.A.; Estévez, J.; Vanschoren, J.; García-Marín, A.P. AgroML: An Open-Source Repository to Forecast Reference Evapotranspiration in Different Geo-Climatic Conditions Using Machine Learning and Transformer-Based Models. *Agronomy* **2022**, *12*, 656. [[CrossRef](#)]
24. Fan, J.; Yue, W.; Wu, L.; Zhang, F.; Cai, H.; Wang, X.; Lu, X.; Xiang, Y. Evaluation of SVM, ELM and Four Tree-Based Ensemble Models for Predicting Daily Reference Evapotranspiration Using Limited Meteorological Data in Different Climates of China. *Agric. For. Meteorol.* **2018**, *263*, 225–241. [[CrossRef](#)]
25. Liu, X.; Wu, L.; Zhang, F.; Huang, G.; Yan, F.; Bai, W. Splitting and Length of Years for Improving Tree-Based Models to Predict Reference Crop Evapotranspiration in the Humid Regions of China. *Water* **2021**, *13*, 3478. [[CrossRef](#)]
26. Wu, Z.; Cui, N.; Gong, D.; Zhu, F.; Xing, L.; Zhu, B.; Chen, X.; Wen, S.; Liu, Q. Simulation of Daily Maize Evapotranspiration at Different Growth Stages Using Four Machine Learning Models in Semi-Humid Regions of Northwest China. *J. Hydrol.* **2022**, *617*, 128947. [[CrossRef](#)]
27. Zhou, Z.; Zhao, L.; Lin, A.; Qin, W.; Lu, Y.; Li, J.; Zhong, Y.; He, L. Exploring the Potential of Deep Factorization Machine and Various Gradient Boosting Models in Modeling Daily Reference Evapotranspiration in China. *Arab. J. Geosci.* **2021**, *13*, 1287. [[CrossRef](#)]
28. Wu, L.; Peng, Y.; Fan, J.; Wang, Y. Machine Learning Models for the Estimation of Monthly Mean Daily Reference Evapotranspiration Based on Cross-Station and Synthetic Data. *Hydrol. Res.* **2019**, *50*, 1730–1750. [[CrossRef](#)]
29. Fan, J.; Ma, X.; Wu, L.; Zhang, F.; Yu, X.; Zeng, W. Light Gradient Boosting Machine: An Efficient Soft Computing Model for Estimating Daily Reference Evapotranspiration with Local and External Meteorological Data. *Agric. Water Manag.* **2019**, *225*, 105758. [[CrossRef](#)]
30. Wu, T.; Zhang, W.; Jiao, X.; Guo, W.; Hamoud, Y.A. Comparison of Five Boosting-Based Models for Estimating Daily Reference Evapotranspiration with Limited Meteorological Variables. *PLoS ONE* **2020**, *15*, e0235324. [[CrossRef](#)] [[PubMed](#)]
31. Zhang, H.; Meng, F.; Xu, J.; Liu, Z.; Meng, J. Evaluation of Machine Learning Models for Daily Reference Evapotranspiration Modeling Using Limited Meteorological Data in Eastern Inner Mongolia, North China. *Water* **2022**, *14*, 2890. [[CrossRef](#)]
32. Ferreira, L.B.; da Cunha, F.F. New Approach to Estimate Daily Reference Evapotranspiration Based on Hourly Temperature and Relative Humidity Using Machine Learning and Deep Learning. *Agric. Water Manag.* **2020**, *234*, 106113. [[CrossRef](#)]

33. Mokari, E.; DuBois, D.; Samani, Z.; Mohebzadeh, H.; Djaman, K. Estimation of Daily Reference Evapotranspiration with Limited Climatic Data Using Machine Learning Approaches across Different Climate Zones in New Mexico. *Theor. Appl. Climatol.* **2022**, *147*, 575–587. [[CrossRef](#)]
34. Wu, T.; Zhang, W.; Jiao, X.; Guo, W.; Alhaj Hamoud, Y. Evaluation of Stacking and Blending Ensemble Learning Methods for Estimating Daily Reference Evapotranspiration. *Comput. Electron. Agric.* **2021**, *184*, 106039. [[CrossRef](#)]
35. Yan, S.; Wu, L.; Fan, J.; Zhang, F.; Zou, Y.; Wu, Y. A Novel Hybrid WOA-XGB Model for Estimating Daily Reference Evapotranspiration Using Local and External Meteorological Data: Applications in Arid and Humid Regions of China. *Agric. Water Manag.* **2021**, *244*, 106594. [[CrossRef](#)]
36. Maroufpoor, S.; Bozorg-Haddad, O.; Maroufpoor, E. Reference Evapotranspiration Estimating Based on Optimal Input Combination and Hybrid Artificial Intelligent Model: Hybridization of Artificial Neural Network with Grey Wolf Optimizer Algorithm. *J. Hydrol.* **2020**, *588*, 125060. [[CrossRef](#)]
37. Dong, J.; Liu, X.; Huang, G.; Fan, J.; Wu, L.; Wu, J. Comparison of Four Bio-Inspired Algorithms to Optimize KNEA for Predicting Monthly Reference Evapotranspiration in Different Climate Zones of China. *Comput. Electron. Agric.* **2021**, *186*, 106211. [[CrossRef](#)]
38. Devendra, C.; Thomas, D. Crop–Animal Systems in Asia: Importance of Livestock and Characterisation of Agro-Ecological Zones. *Agric. Syst.* **2002**, *71*, 5–15. [[CrossRef](#)]
39. Mandal, D.; Mandal, C.; Singh, S. Delineating Agro-Ecological Regions. *ICAR-NBSSLUIP Technol.* **2016**, 1–8.
40. Allen, R.G.; Pereira, L.S.; Raes, D.; Smith, M. Crop Evapotranspiration-Guidelines for Computing Crop Water Requirements-FAO Irrigation and Drainage Paper 56. *FAO Rome* **1998**, *300*, D05109.
41. Tabari, H.; Grismer, M.E.; Trajkovic, S. Comparative Analysis of 31 Reference Evapotranspiration Methods under Humid Conditions. *Irrig. Sci.* **2013**, *31*, 107–117. [[CrossRef](#)]
42. Xystrakis, F.; Matzarakis, A. Evaluation of 13 Empirical Reference Potential Evapotranspiration Equations on the Island of Crete in Southern Greece. *J. Irrig. Drain. Eng.* **2011**, *137*, 211–222. [[CrossRef](#)]
43. Rosenberry, D.O.; Stannard, D.I.; Winter, T.C.; Martinez, M.L. Comparison of 13 Equations for Determining Evapotranspiration from a Prairie Wetland, Cottonwood Lake Area, North Dakota, USA. *Wetlands* **2004**, *24*, 483–497. [[CrossRef](#)]
44. Bourletsikas, A.; Argyrokastritis, I.; Proutsos, N. Comparative Evaluation of 24 Reference Evapotranspiration Equations Applied on an Evergreen-Broadleaved Forest. *Hydrol. Res.* **2017**, *49*, 1028–1041. [[CrossRef](#)]
45. Breiman, L. Random Forests. *Mach. Learn.* **2001**, *45*, 5–32. [[CrossRef](#)]
46. Smith, P.F.; Ganesh, S.; Liu, P. A Comparison of Random Forest Regression and Multiple Linear Regression for Prediction in Neuroscience. *J. Neurosci. Methods* **2013**, *220*, 85–91. [[CrossRef](#)] [[PubMed](#)]
47. Misra, S.; Li, H. Chapter 9—Noninvasive Fracture Characterization Based on the Classification of Sonic Wave Travel Times. In *Machine Learning for Subsurface Characterization*; Misra, S., Li, H., He, J., Eds.; Gulf Professional Publishing: Houston, TX, USA, 2020; pp. 243–287. ISBN 978-0-12-817736-5.
48. Chen, T.; He, T.; Benesty, M.; Khotilovich, V.; Tang, Y.; Cho, H.; Chen, K. Xgboost: Extreme Gradient Boosting. In *R Package; Version 04-2*; R Foundation for Statistical Computing: Vienna, Austria, 2015; Volume 1, pp. 1–4.
49. Friedman, J.H. Greedy Function Approximation: A Gradient Boosting Machine. *Ann. Stat.* **2001**, *29*, 1189–1232. [[CrossRef](#)]
50. Al Daoud, E. Comparison between XGBoost, LightGBM and CatBoost Using a Home Credit Dataset. *Int. J. Comput. Inf. Eng.* **2019**, *13*, 6–10.
51. Ke, G.; Meng, Q.; Finley, T.; Wang, T.; Chen, W.; Ma, W.; Ye, Q.; Liu, T.-Y. LightGBM: A Highly Efficient Gradient Boosting Decision Tree. In *Proceedings of the Advances in Neural Information Processing Systems, Long Beach, CA, USA, 4–9 December 2017*; Curran Associates, Inc.: Red Hook, NY, USA, 2017; Volume 30.
52. Mirjalili, S.; Mirjalili, S.M.; Lewis, A. Grey Wolf Optimizer. *Adv. Eng. Softw.* **2014**, *69*, 46–61. [[CrossRef](#)]
53. Sweidan, A.H.; El-Bendary, N.; Hassani, A.E.; Hegazy, O.M.; Mohamed, A.E. Water Quality Classification Approach Based on Bio-Inspired Gray Wolf Optimization. In *Proceedings of the 2015 7th International Conference of Soft Computing and Pattern Recognition (SoCPaR), Fukuoka, Japan, 13–15 November 2015*; pp. 1–6.
54. Faris, H.; Aljarah, I.; Al-Betar, M.A.; Mirjalili, S. Grey Wolf Optimizer: A Review of Recent Variants and Applications. *Neural Comput. Appl.* **2018**, *30*, 413–435. [[CrossRef](#)]
55. Mohammadi, B.; Guan, Y.; Aghelpour, P.; Emamgholizadeh, S.; Pillco Zola, R.; Zhang, D. Simulation of Titicaca Lake Water Level Fluctuations Using Hybrid Machine Learning Technique Integrated with Grey Wolf Optimizer Algorithm. *Water* **2020**, *12*, 3015. [[CrossRef](#)]
56. Sharma, I.; Kumar, V.; Sharma, S. A Comprehensive Survey on Grey Wolf Optimization. *Recent Adv. Comput. Sci. Commun. Former. Recent Pat. Comput. Sci.* **2022**, *15*, 323–333.
57. Feng, Y.; Cui, N.; Zhao, L.; Hu, X.; Gong, D. Comparison of ELM, GANN, WNN and Empirical Models for Estimating Reference Evapotranspiration in Humid Region of Southwest China. *J. Hydrol.* **2016**, *536*, 376–383. [[CrossRef](#)]
58. He, H.; Liu, L.; Zhu, X. Optimization of Extreme Learning Machine Model with Biological Heuristic Algorithms to Estimate Daily Reference Evapotranspiration in Hetao Irrigation District of China. *Eng. Appl. Comput. Fluid Mech.* **2022**, *16*, 1939–1956. [[CrossRef](#)]
59. Heramb, P.; Kumar Singh, P.; Ramana Rao, K.V.; Subeesh, A. Modelling Reference Evapotranspiration Using Gene Expression Programming and Artificial Neural Network at Pantnagar, India. *Inf. Process. Agric.* **2022**, *in press*. [[CrossRef](#)]

60. Despotovic, M.; Nedic, V.; Despotovic, D.; Cvetanovic, S. Review and Statistical Analysis of Different Global Solar Radiation Sunshine Models. *Renew. Sustain. Energy Rev.* **2015**, *52*, 1869–1880. [[CrossRef](#)]
61. Zhu, B.; Feng, Y.; Gong, D.; Jiang, S.; Zhao, L.; Cui, N. Hybrid Particle Swarm Optimization with Extreme Learning Machine for Daily Reference Evapotranspiration Prediction from Limited Climatic Data. *Comput. Electron. Agric.* **2020**, *173*, 105430. [[CrossRef](#)]
62. Pandey, P.K.; Dabral, P.P.; Pandey, V. Evaluation of Reference Evapotranspiration Methods for the Northeastern Region of India. *Int. Soil Water Conserv. Res.* **2016**, *4*, 52–63. [[CrossRef](#)]
63. Üneş, F.; Kaya, Y.Z.; Mamak, M. Daily Reference Evapotranspiration Prediction Based on Climatic Conditions Applying Different Data Mining Techniques and Empirical Equations. *Theor. Appl. Climatol.* **2020**, *141*, 763–773. [[CrossRef](#)]
64. Salam, R.; Islam, A.R.M.T. Potential of RT, Bagging and RS Ensemble Learning Algorithms for Reference Evapotranspiration Prediction Using Climatic Data-Limited Humid Region in Bangladesh. *J. Hydrol.* **2020**, *590*, 125241. [[CrossRef](#)]
65. Huang, G.; Wu, L.; Ma, X.; Zhang, W.; Fan, J.; Yu, X.; Zeng, W.; Zhou, H. Evaluation of CatBoost Method for Prediction of Reference Evapotranspiration in Humid Regions. *J. Hydrol.* **2019**, *574*, 1029–1041. [[CrossRef](#)]

Disclaimer/Publisher’s Note: The statements, opinions and data contained in all publications are solely those of the individual author(s) and contributor(s) and not of MDPI and/or the editor(s). MDPI and/or the editor(s) disclaim responsibility for any injury to people or property resulting from any ideas, methods, instructions or products referred to in the content.